

Radiation Problem in Transplanckian Scattering

Paolo Lodone and Slava Rychkov

Scuola Normale Superiore and INFN, Pisa, Italy

Abstract

We investigate hard radiation emission in small-angle transplanckian scattering. We show how to reduce this problem to a quantum field theory computation in a classical background (gravitational shock wave). In momentum space, the formalism is similar to the flat-space light cone perturbation theory, with shock wave crossing vertices added. In the impact parameter representation, the radiating particle splits into a multi-particle virtual state, whose wavefunction is then multiplied by individual eikonal factors.

As a phenomenological application, we study QCD radiation in transplanckian collisions of TeV-scale gravity models. We derive the distribution of initial state radiation gluons, and find a suppression at large transverse momenta with respect to the standard QCD result. This is due to rescattering events, in which the quark and the emitted gluon scatter coherently. Interestingly, the suppression factor depends on the number of extra dimensions and provides a new experimental handle to measure this number. We evaluate the leading-log corrections to partonic cross-sections due to the initial state radiation, and prove that they can be absorbed into the hadronic PDF. The factorization scale should then be chosen in agreement with an earlier proposal of Emparan, Masip, and Rattazzi.

In the future, our methods can be applied to the gravitational radiation in transplanckian scattering, where they can go beyond the existing approaches limited to the soft radiation case.

1 Introduction

Scattering at center-of-mass (CM) energies exceeding the quantum gravity scale (transplanckian scattering, or *T-scattering*, for short) is an exotic process of significant theoretical interest. In particular, it provides a laboratory to study the black hole information loss paradox. Microscopic black hole formation and its subsequent evaporation is expected for impact parameters b of the order of the Schwarzschild radius R_S of a black hole of mass \sqrt{s} [1],[2],[3],[4]. The detailed description of how this happens depends on the unknown underlying theory of quantum gravity and is at present out of reach. On the other hand, large impact parameters $b \gg R_S$ correspond to elastic small-angle scattering, whose amplitude can be predicted on the basis of General Relativity alone. It is given by eikonized single-graviton exchange [1],[5],[6],[7]. Computing the corrections in b/R_S to the elastic scattering, one hopes to learn about the strong inelastic dynamics at $b \sim R_S$ [8],[9],[10],[11],[12].

T-scattering is also interesting phenomenologically. If large extra dimension scenarios of TeV-scale gravity [13] are realized in Nature, this process could be observed at the LHC and other future colliders [14],[15], as well as in collisions of high-energy cosmic neutrinos with atmospheric nucleons [16],[17]. In these scenarios the total T-scattering cross section is finite, grows with energy, and is dominated by calculable small-angle scattering between partonic constituents [17],[15], see Fig. 1. The subleading black hole production cross section at present can only be estimated from geometrical arguments.

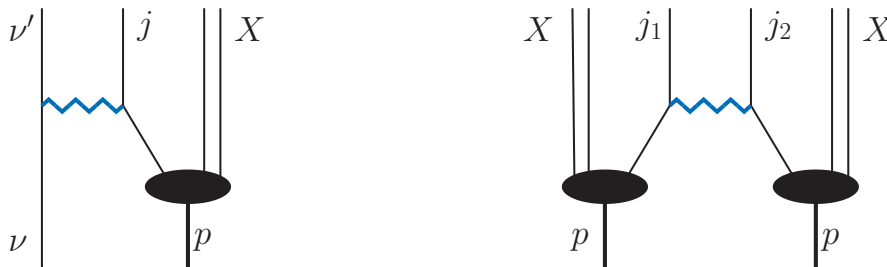


Figure 1: *The νp T-scattering in cosmic ray physics (left) and the pp T-scattering at the LHC (right). In both cases the dominant process is small-angle elastic scattering between partons, giving jet(s)+anything in the final state. The zigzag line denotes the eikonal $2 \rightarrow 2$ scattering amplitude.*

In spite of the small scattering angle, the typical momentum transfer in these scattering events is well above the QCD scale, and the typical impact parameter is much smaller than the proton

size, which sets the typical distance between two uncorrelated partons inside the proton. It is unlikely that a multiple parton interaction, Fig. 2, will occur in the same T-scattering. Thus it is clear that the partonic picture should be applicable at leading order in the QCD coupling. In other words, we can compute the total cross section via a convolution of the partonic cross section and the parton distribution functions (PDF) $f(x, \mu_F^2)$.

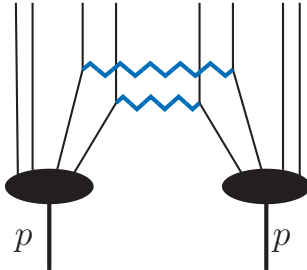


Figure 2: *Multiple partonic interactions, in which more than one pair of partons exchange gravitons, are suppressed. This is because the eikonal phase vanishes very quickly with the transverse separation, and it is unlikely to find a second pair of partons for which this phase is large.*

Several interesting questions arise when one tries to think what happens beyond the leading order. For example, it's not known how to treat events of the type shown in Fig. 3, where one of the colliding partons (say a quark) radiates a gluon just before the collision. Now the quark-gluon separation is not necessarily large, and the pair may scatter coherently. What is the correct description of such *rescattering* processes, and what is the resulting effect on the total T-scattering cross section?

A related question is: which factorization scale μ_F should we choose in the computation of the total cross section? As is well known, QCD-initiated processes have significant higher-order logarithmic corrections, associated with the collinear QCD radiation off initial partons. By choosing μ_F appropriately, these corrections can and should be reabsorbed into the PDF. As we will see below, the familiar choice $\mu_F^2 \sim -t$ is likely not the right one for the T-scattering. If so, we would like to see this explicitly.

The purpose of this paper is to answer the above-mentioned questions. We will be focusing on the QCD radiation since it is the dominant phenomenological effect due to the relative largeness of α_s . However, our methods are equally applicable to the radiation of photons or any other spin 1 gauge bosons. We also hope that these methods may later prove useful in the more complicated

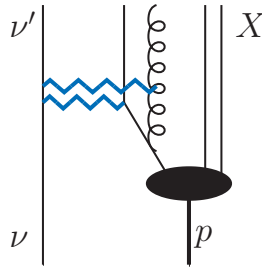


Figure 3: *Initial state radiation processes, when a quark emits a gluon just before participating in T-scattering, are expected to play a role. They give logarithmic corrections to the cross section, which determine the optimal factorization scale μ_F of the process.*

problem of *gravitational* radiation emitted in T-scattering, and in particular to provide an alternative to the existing computations which are limited to the case when the emitted radiation is *soft* [8],[18].

The paper is organized as follows. In Section 2 we review the eikonalization of small-angle $2 \rightarrow 2$ partonic scattering amplitude, following [17],[15]. To keep close contact with phenomenology, we work in the context of large extra dimension scenarios with the quantum gravity scale around a TeV. A key feature of the extra-dimensional situation with n compactified dimensions is the appearance of a new length scale b_c , which sets the range of a typical T-scattering interaction. In D -dimensional Planck units, $D = 4 + n$, we have

$$b_c \sim s^{1/n}, \quad R_S \sim s^{1/[2(n+1)]},$$

so that $b_c \gg R_S$ in the deep transplanckian regime $\sqrt{s} \gg 1$. We also present an alternative computation of the $2 \rightarrow 2$ amplitude, based on generalizing to D dimensions the early idea of 't Hooft [1], who considered the small-angle T-scattering by solving the Klein-Gordon equation for one particle propagating in the classical gravitational field of the other particle.

In Section 3 we start discussing small-angle T-scattering with hadronic initial states, as in Fig. 1, in which QCD effects are expected to play a role. According to the existing proposal of Emparan, Masip and Rattazzi [17], the total cross section for these processes must be computed with the following prescription for the PDF scale μ_F :

$$\mu_F(q) = \begin{cases} q & \text{if } q < b_c^{-1}, \\ q^{\frac{1}{n+1}} (b_c^{-1})^{\frac{n}{n+1}} & \text{if } q > b_c^{-1}, \end{cases} \quad (1.1)$$

where $q \equiv \sqrt{-t}$. For sufficiently high momentum transfers this deviates from the familiar pre-

scription $\mu_F \simeq q$. An intuitive justification for this scale in terms of the typical impact parameter was given in [17], but we would like to check it via a direct computation.

The first step is to be able to evaluate the amplitude for small-angle T-scattering accompanied by collinear QCD radiation. In the resummation approach [17],[15], this computation seems prohibitively difficult even for one-gluon emission. Indeed, the eikonal amplitude for quark-quark T-scattering is a sum of an infinite number of crossed ladder graviton exchanges. The outgoing gluon may be attached anywhere on the quark lines, both external and internal. Moreover, in the $q \rightarrow q + g$ splitting, the emitted near-collinear gluon is not necessarily soft, and thus may also exchange gravitons. The number of diagrams to resum skyrockets.

't Hooft's approach is a much better starting point. As we point out, it can be easily 'upgraded' to the case when radiation is present, provided that only one of the two colliding particles radiates. This covers completely lepton-quark scattering and is an important special case for quark-quark scattering. The idea is very simple. In the $2 \rightarrow 2$ scattering, 't Hooft treated one particle classically, the other one quantum mechanically. The only new twist is to allow the quantum particle to radiate. In other words, we should treat the non-radiating parton classically, while the radiating parton *and the gluonic radiation field with which it interacts* quantum mechanically.

This trick reduces the problem to a quantum field theory computation in the classical gravitational background produced by a relativistic point particle, the Aichelburg-Sexl (AS) shock wave [19]. In Section 4 we develop the necessary formalism. We first consider the simplest perturbative quantum field theory in the AS background: a scalar field with cubic self-interactions. We introduce a diagram technique for computing arbitrary transition amplitudes in this theory, which turns out to be closely related to the standard rules of light-cone perturbation theory in flat space. We then explain the changes necessary for the gluon field and for the scalar-gluon interactions, and compute the one-gluon emission amplitude as an example.

Notice that while fermionic matter fields can be considered analogously, we do not include them in this work in order to keep technical details to a minimum. Thus we stick to a toy model in which the partonic constituents of colliding hadron(s) are scalars.

Armed with the knowledge of gluon emission amplitudes, in Section 5 we attack the question of QCD corrections to T-scattering. For definiteness and simplicity, we consider the gravitational analogue of the DIS: a transplanckian electron-proton collision. The observable is the total cross section as a function of the Bjorken x and the transverse momentum transfer \mathbf{q} , in the small-angle region $|\mathbf{q}| \ll \sqrt{s}$. At leading order (LO) in the QCD coupling α_s , the partons scatter elastically on the electron (no gluon emission). At next-to-leading order (NLO), we demonstrate

the appearance of logarithmic corrections whose scale is precisely the $\mu_F(q)$ from Eq. (1.1). We find that the cross section factorizes, in the sense that these logarithms appear multiplied by the DGLAP splitting functions, and can be reabsorbed into the PDFs. Finally, we are able to show that this factorization holds to all orders in α_s , in the leading-logarithm approximation (LLA).

Our computation gives an explicit check for the validity of the partonic picture for the T-scattering. Moreover, it gives an interesting and unexpected explanation for why the PDF scale deviates from the usual $\mu_F \sim q$. It turns out that rescatterings like in Fig. 3 *suppress the initial state QCD radiation at transverse momenta* $q \gtrsim b_c^{-1}$. As a result the transverse momentum distribution of emitted gluons has the form:

$$\frac{dN}{d^2\mathbf{q}} = f(q) \left(\frac{dN}{d^2\mathbf{q}} \right)_0, \quad (1.2)$$

where $(dN/d^2\mathbf{q})_0 \sim 1/\mathbf{q}^2$ is the standard distribution without rescattering, and $f(q)$ is a function interpolating between 1 for $q \ll b_c^{-1}$ and $1/(n+1)$ for $q \gg b_c^{-1}$. Logarithmic corrections to the cross section are obtained, as usual, by integrating Eq. (1.2) over the gluon phase space, and the scale of these logarithms is a geometric mean of q and b_c^{-1} as in Eq. (1.1).

Notice that one could imagine other distributions giving rise to $\log \mu_F(q)$, for example the standard $1/\mathbf{q}^2$ with a sharp cutoff at b_*^{-1} . In this sense Eq. (1.2) contains more information than the identification of the correct factorization scale. The predicted suppression of the initial state radiation is n -dependent and could in principle be used to determine the number of extra dimensions.

A crucial insight into the physics of radiative processes is obtained by going into the impact parameter representation. In this picture, we find that the scattering is described via a multi-particle wavefunction of the virtual state (parton+radiated quanta), which is multiplied by individual eikonal factors when crossing the shock wave. This interpretation suggests a possible generalization of our formalism to the case when both colliding partons radiate, which we discuss in Section 6.

In conclusion, this work shows that factorization holds for QCD effects in T-scattering, and that the factorization scale has a nontrivial dependence on q^2 , in agreement with the earlier proposal of Ref. [17]. The novelty is that we arrive at these results by a concrete computation, and that we derive the modified distribution of the initial state radiation due to rescattering effects. The new distribution should be now incorporated into a ‘transplanckian parton shower algorithm’, to be used in Monte-Carlo simulations of T-scattering. We will come back to this issue in a future publication.

2 Review of the eikonal approach to T-scattering

In this section we review the basics of small angle T-scattering in the eikonal approximation. We will work within the large flat extra dimensions scenario of TeV-scale gravity [13], see [20] for the current experimental constraints.

Consider then two transplanckian massless Standard Model (SM) particles, thus confined to the SM 3-brane, which scatter due to the D -dimensional gravitational field, $D = 4 + n$, n being the number of large extra dimensions, $n \geq 2$ for phenomenological reasons. For now we ignore all interactions except for gravity. In particular, we suppose that the colliding particles are not charged, and thus cannot emit photons or gluons. We are interested in the scattering amplitude for small momentum transfer $-t/s \ll 1$. In this regime gravitational radiation is also suppressed (see [15]), and we have elastic $2 \rightarrow 2$ scattering.

2.1 Resummation

The most direct way to compute the amplitude is by resumming the crossed ladder graviton exchange diagrams [17],[15], see Fig. 4. For small momentum transfer, exchanged gravitons are soft, and well-known simplifications occur in the vertices and the intermediate state propagators, allowing the resummation. The first term in the series, the one-graviton exchange, is given by

$$\mathcal{A}_{\text{Born}}(\mathbf{q}) = -\frac{s^2}{M_D^{n+2}} \int \frac{d^n l}{\mathbf{q}^2 + l^2}, \quad (2.1)$$

where \mathbf{q} is the momentum transfer, which lies mostly in the direction transverse to the beam: $t \approx -\mathbf{q}^2$. The D -dimensional Planck scale $M_D \sim 1$ TeV is normalized as in [15],[20]. The divergent integral over the extra dimensional momentum l needs to be treated properly; see below. The second term in the series, the sum of two one-loop diagrams, turns out to be equal to a convolution of two Born amplitudes:

$$\mathcal{A}_{\text{1-loop}}(\mathbf{q}) = \frac{i}{4s} \int \frac{d^2 \mathbf{k}}{(2\pi)^2} A_{\text{Born}}(\mathbf{k}) A_{\text{Born}}(\mathbf{q} - \mathbf{k}),$$

and this pattern continues to higher orders. As a result the series can be summed by going to the impact parameter representation. The amplitude acquires the eikonal form:

$$\mathcal{A}_{\text{eik}}(\mathbf{q}) = \mathcal{A}_{\text{Born}} + \mathcal{A}_{\text{1-loop}} + \dots = -2is \int d^2 \mathbf{b} e^{-i\mathbf{q}\cdot\mathbf{b}} (e^{i\chi} - 1), \quad (2.2)$$

with the eikonal phase χ given by the Fourier transform of the Born amplitude in the transverse plane:

$$\chi(\mathbf{b}) = \frac{1}{2s} \int \frac{d^2 \mathbf{q}}{(2\pi)^2} e^{i\mathbf{q}\cdot\mathbf{b}} A_{\text{Born}}(\mathbf{q}).$$

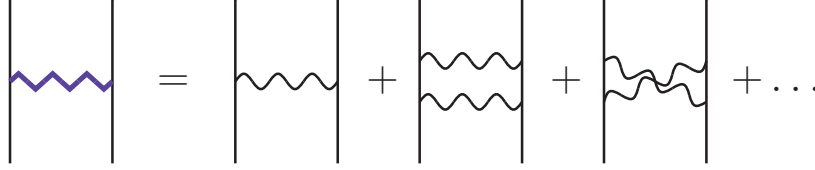


Figure 4: *The $2 \rightarrow 2$ small angle T-scattering amplitude is given by a sum of crossed-ladder graviton exchanges.*

To evaluate the eikonal phase, we need to regulate the divergent Born amplitude (2.1). In [15], dimensional regularization was used, and it was argued that since the subtracted divergent terms are local, they do not affect the small angle scattering amplitude¹. The eikonal phase was found to be:

$$\chi(\mathbf{b}) = \left(\frac{b_c}{|\mathbf{b}|} \right)^n, \quad b_c = \frac{1}{M_D} \left[\frac{(4\pi)^{\frac{n}{2}-1} \Gamma(n/2)}{2} \right]^{1/n} \left(\frac{s}{M_D^2} \right)^{1/n}. \quad (2.3)$$

The corresponding amplitude is then given by:

$$\mathcal{A}_{\text{eik}} = 4\pi s b_c^2 F_n(b_c |\mathbf{q}|),$$

$$F_n(y) = -i \int_0^\infty dx x J_0(xy) [e^{ix^{-n}} - 1]. \quad (2.4)$$

The functions $F_n(y)$ are plotted in Fig. 5 (see also Fig. 2 of [15]). Their most salient features are as follows. At moderate $y \lesssim 1$, we have $F_n(y) = \mathcal{O}(1)$,² the integral (2.4) receiving contributions from $x \sim 1$. On the other hand, for $y \gg 1$ the integral has a saddle point at $x_* = (n/y^n)^{\frac{1}{n+1}} \ll 1$, and the amplitude decays:

$$|F_n(y)| \simeq \frac{n^{\frac{1}{n+1}}}{\sqrt{n+1}} y^{-\frac{n+2}{n+1}} \quad (y \gg 1).$$

The appearance of the scale b_c is a peculiar feature of T-scattering for $n > 0$. Since the amplitude is the largest in the region $y \lesssim 1$, a typical scattering will have $|\mathbf{q}| \lesssim b_c^{-1}$. Yet a classical particle trajectory for these \mathbf{q} is undefined, all impact parameters $b \sim b_c$ contributing to the scattering. On the other hand, for $b_c |\mathbf{q}| \gg 1$ ($y \gg 1$) the scattering is dominated by a characteristic impact parameter $b_* = b_c x_*$, corresponding to the above saddle point. In this

¹This was later confirmed in [21] by using in (2.1) a physical regulator $\exp(-k^2 w^2)$, with w interpreted as an effective width of the SM brane, $w \sim \text{TeV}^{-1}$. It was found that the resulting eikonal phase coincides with (2.3) for $b \gtrsim w$, while for $b \lesssim w$ it varies slowly (logarithmically). The eikonal amplitude then indeed agrees with (2.4) in the small scattering angle region. The same conclusion was also reached in [22] using a sharp cutoff.

²For $n = 2$ there is mild logarithmic growth.

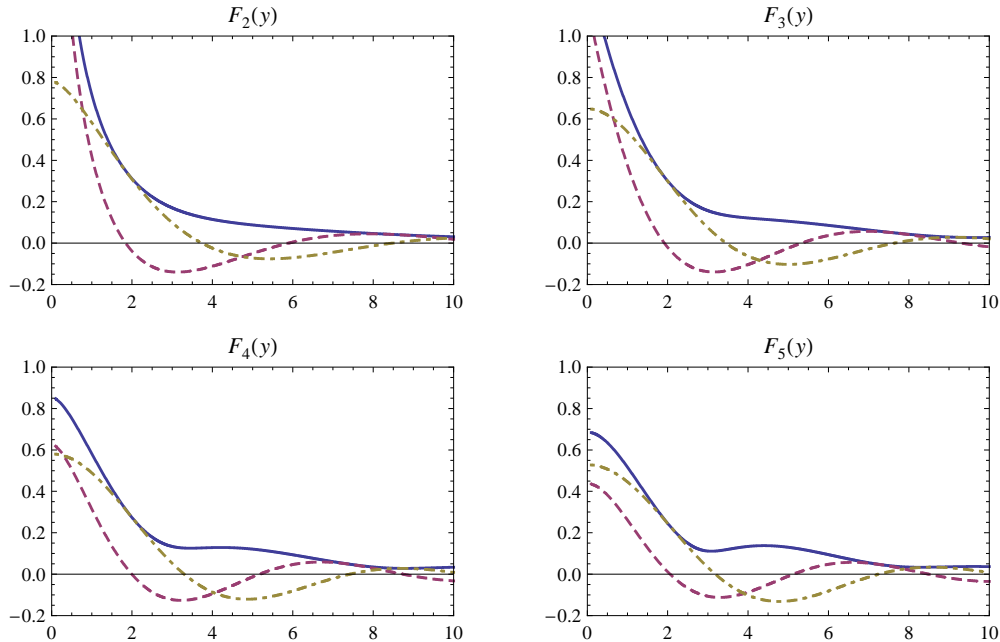


Figure 5: The functions $F_n(y)$ for $n = 2, 3, 4, 5$: absolute value (solid), real part (dashed), imaginary part (dot-dashed). Notice that $\Im F_n(0) < \infty$ for all $n \geq 2$, implying finite total cross section. On the other hand, $\Re F_n(0) < \infty$ for all $n \geq 3$. See [15].

case the particle trajectory is well defined and the T-scattering is truly semiclassical, with many gravitons being exchanged.

2.2 't Hooft's method

An alternative computation of the small angle T-scattering amplitude can be given using a method due to 't Hooft [1], originally formulated in four dimensions. In this approach, particle B scatters on the classical gravitational field created by particle A . In other words, particle A is treated as a classical point particle, while particle B is treated quantum-mechanically.

Consider then the gravitational field of a relativistic classical point particle A of energy E_A propagating in the positive z direction. This field is the D -dimensional generalization of the AS [19] shock wave:

$$ds^2 = -dx^+ dx^- + \Phi(x_\perp) \delta(x^-) (dx^-)^2 + dx_\perp^2. \quad (2.5)$$

Here $x^\pm = t \pm z$, while x_\perp denotes $D - 2$ transverse directions. Einstein's equations with the

lightlike source

$$T_{--} = E_A \delta(x^-) \delta^{(D-2)}(x_\perp)$$

reduce to one linear equation for the shock wave profile Φ :

$$-\partial_\perp^2 \Phi = 16\pi G_D E_A \delta^{(D-2)}(x_\perp). \quad (2.6)$$

The solution of this equation coincides with the eikonal phase (2.3) per unit of particle B energy:

$$\Phi(x_\perp) = E_B^{-1} \chi(x_\perp). \quad (2.7)$$

The right-moving particle B is confined to the SM 3-brane, and its wavefunction solves the Klein-Gordon equation in the metric induced on the brane by the shock wave (2.5). At $x^- < 0$ the wavefunction is a standard plane wave

$$\phi(x) = \exp(ip_B \cdot x) = \exp(-iE_B x^+).$$

The metric (2.5) has a strong discontinuity at $x^- = 0$. To solve the Klein-Gordon equation across the discontinuity, it is convenient to make a coordinate transformation [3],[23]

$$\begin{aligned} x^- &= \tilde{x}^-, \\ x^+ &= \tilde{x}^+ + \theta(x^-) \Phi(\tilde{x}_i) + x^- \theta(x^-) \frac{(\partial \Phi(\tilde{x}_i))^2}{4}, \\ x_i &= \tilde{x}_i + \frac{x^-}{2} \theta(x^-) \partial_i \Phi(\tilde{x}_i). \end{aligned} \quad (2.8)$$

In the \tilde{x} coordinates the metric is continuous across $x^- = 0$. When crossing the shock wave, the wavefunction remains continuous in these coordinates. This means that for small positive x^- we have:

$$\phi(\tilde{x}) = \exp(-iE_B \tilde{x}^+) = \exp[-iE_B(x^+ - \Phi(\mathbf{x}))]. \quad (2.9)$$

The \mathbf{x} -dependent shift of the x^+ coordinate has a well-known classical origin: it is related to the time delay experienced by geodesics crossing the AS shock wave, see Fig. 6.³

We now see from (2.9) that the wavefunction immediately before and after the collision is related by a pure phase factor $\exp(iE_B \Phi(\mathbf{x}))$, which via (2.7) is identical with the eikonal phase

³We would like to stress the *auxiliary* character of the \tilde{x} coordinates, in which the metric is not manifestly flat for $\tilde{x}^- > 0$, nor even manifestly asymptotically flat, which makes these coordinates unsuitable for defining asymptotic outgoing states. The asymptotic states should be described in the x coordinates, that's why in the last equation in (2.9) we reverted to them.

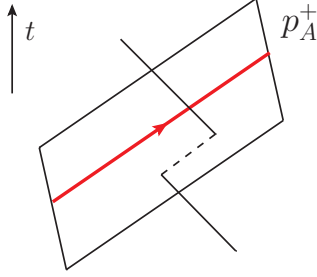


Figure 6: *The gravitational field of particle A (the AS shock wave) is concentrated on the null plane $x^- = 0$. Geodesics crossing this field experience an \mathbf{x} -dependent shift of the x^+ coordinate. This is the same shift as in Eq. (2.9).*

factor in (2.3). An alternative derivation, by directly solving the Klein-Gordon equation, is given in Appendix A.

Thus, 't Hooft's method is equivalent to the resummation. This is not surprising, because the external field approximation in quantum field theory resums precisely crossed ladder diagrams [24]. The AS shock wave is a solution to both linearized gravity and the full nonlinear Einstein's equations. In retrospect, this explains why the diagrams in which gravitons emitted by particles A and B interact did not have to be taken into account in the resummation method. See [7] for a detailed discussion and comparison of the two methods in $D = 4$.

Still, an attentive reader will notice two small differences between the two results. First, Eq. (2.3) contains -1 under the integral sign, while 't Hooft's method gives a pure phase. This is the usual difference between the S- and T-matrices, $S = 1 + iT$. Second, the amplitude (2.3) is relativistically normalized, while in the new derivation normalization needs yet to be determined.

Modulo the normalization issue (which will be resolved in Section 4.1 below), the power of 't Hooft's method relative to the resummation is quite evident. The eikonal phase is given a simple physical interpretation—it is related to the time delay experienced by geodesics upon crossing the shock wave. The exponential factor $e^{i\chi}$ emerges as a whole rather than by summing infinitely many individually large terms.

3 T-scattering with hadrons: intuition and questions

If TeV-scale gravity is the way of Nature, then transplanckian collisions may be within the energy reach of the LHC. Moreover, transplanckian collisions may be constantly happening in the

atmosphere, between the atmospheric nucleons and high-energy cosmic rays ($\sqrt{s} \sim 10^6$ GeV for $E_{cr} \sim 10^{11}$ GeV of the order of the GZK cutoff). In case of cosmic ray neutrinos this signal could actually be observable.

Since protons are not elementary particles, the theory of small angle T-scattering from Section 2 should be applied instead to $2 \rightarrow 2$ collisions between the partonic constituents. Notice that since we are dealing with CM energies well over a TeV, the typical momentum transfers will be hard compared to the QCD scale, even though the scattering angle has to be small for the eikonal approximation to be valid. Thus the collision resolves the internal structure of the proton(s), and the partonic picture is applicable [17].

Viewed another way, when two protons collide, there is a phase factor $\sim \Phi(\mathbf{x} - \mathbf{y})$ for each pair of partons moving in the opposite directions, see Fig. 2. This factor tends to zero rapidly at transverse separations $|\mathbf{x} - \mathbf{y}| \gg b_c$, where $b_c \sim (100 \text{ GeV})^{-1}$ for T-scattering at the LHC energies. Since partons are distributed in the disk of radius $(\text{GeV})^{-1} \gg b_c$, it is unlikely that more than one pair will undergo a hard collision.

We would like to briefly mention which observables one usually computes in phenomenological studies. In νp collisions one is mostly interested in the total interaction cross section as a function of the energy transfer to the proton [17],[22],[25]. We will discuss a similar observable in Section 5 below. On the other hand, in the pp collisions at the LHC one studies two jet final states of high invariant mass, produced at a small angle to the beam [15],[26], see Fig. 1. These jets originate from all possible parton pairs (qq, qg, gg) with the same partonic cross section, the eikonal amplitude being independent of the particle spin. For M_D not much above a TeV, the dijet T-scattering signal turns out to be visible over the QCD background.

So far it may look that from the point of view of QCD, the T-scattering is just like any other hard process. Let us however discuss which parton distribution factorization scale μ_F one should use when evaluating the T-scattering cross sections—a necessary prerequisite for any practical computation.

For the usual hard processes, we are accustomed to the choice $\mu_F \sim |\mathbf{q}|$, but for the T-scattering this turns out to be more subtle. As we discussed in Section 2.1, T-scattering becomes semiclassical in the region of large momentum transfers $|\mathbf{q}| \gg b_c^{-1}$. In this regime, the transverse distance characterizing the process is the typical impact parameter $b_* \sim b_c / (b_c |\mathbf{q}|)^{\frac{1}{n+1}}$ which is *parametrically larger* than $|\mathbf{q}|^{-1}$. It is for this reason that Ref. [17] advocated a hybrid prescription: one should use $\mu_F \sim |\mathbf{q}|$ for $|\mathbf{q}| \lesssim b_c^{-1}$ and switch to $\mu_F \sim b_*^{-1}$ for $|\mathbf{q}| \gg b_c^{-1}$, see Eq. (1.1).⁴

⁴A limiting case of this prescription in the context of black hole production was advocated earlier in the first

For T-scattering at the LHC energies, the factorization scale $\mu_F(q)$ will be hard with respect to the QCD scale as long as the momentum transfer q is hard. This gives a self-consistency check on the proposed picture.⁵

The above is a summary of the current understanding of QCD effects in T-scattering. Clearly, it is based mostly on intuition. We would like to develop a systematic theory of these phenomena. In particular, such a theory should allow to check the factorization scale proposal by a concrete computation. We have to evaluate the leading log corrections to the T-scattering cross section due to the initial state radiation emission, and to show that they can be absorbed into a shift of the PDF factorization scale. Since μ_F is conjectured to have a nontrivial dependence on q , some nontrivial physics is likely to come out.

Two equivalent methods were given in Section 2 to describe T-scattering without radiation. Which one shall we try to generalize to the case when radiation is present?

For the resummation method, generalization does not seem to be easy, not even for the one-gluon emission. Think about infinitely many crossed-ladder diagrams, infinitely many places to attach the gluon line, and the necessity to take into account the gravitational exchanges of the emitted gluon!

For 't Hooft's method, on the other hand, the situation looks hopeful: if only particle B radiates, it is quite clear how to include its radiation. Namely, we should keep working in the classical gravitational background created by particle A , but switch from relativistic quantum mechanics (wavefunctions, the Klein-Gordon equation) to quantum field theory (Green's functions and interaction vertices). We will follow this path and will see that it allows relatively straightforward computations of the gluon emission amplitudes.

Physically, the assumption that particle A does not QCD-radiate is realized if A is a lepton. If both A and B are strongly interacting, one could first compute the radiation off B (taking A classical), then off A (taking B classical). Such an approximation of independent emission is valid for the dominant, collinear, radiation in the usual perturbative processes. For the T-scattering, we will be able to partially justify it below. But first we have to understand well the case of non-radiating A .

Ref. [14].

⁵Notice however that $\mu_F(q)$ is a *decreasing* function of the CM energy, since the typical impact parameter grows with \sqrt{s} . Even for hard momentum transfers, for sufficiently high \sqrt{s} the factorization scale will come down to a GeV, signalling a breakdown of the partonic picture. At even higher CM energies (which are well beyond the range of LHC or even cosmic ray collisions), the proton should interact gravitationally as a point particle.

4 Quantum field theory in the shock wave background

4.1 Scalar field

To compute the QCD radiation accompanying a transplanckian collision, we will replace particle A with the classical background it generates, but will keep particle B and the gluons as quantum fields. Thus we will be doing perturbative QFT computations in the shock wave background. We start with the simplest interacting QFT, the massless ϕ^3 theory:

$$\mathcal{L} = \sqrt{g} \left(\frac{1}{2} g^{\mu\nu} \partial_\mu \phi \partial_\nu \phi - \frac{\lambda}{3!} \phi^3 \right). \quad (4.1)$$

We will describe how to compute transition amplitudes in this theory, and how these are related to the amplitudes in the full theory (i.e. before particle A was replaced by a classical gravitational field).

The $g_{\mu\nu}$ in (4.1) is the 4-dimensional metric obtained by restricting the D -dimensional AS shock wave (2.5) to the SM brane on which both particles and the radiation propagate. We will continue using the coordinates as in (2.5), only restricting the number of x_\perp components from $D - 2$ to 2. Two features make this theory much simpler than it would be for generic curved backgrounds treated in [29]:

1. the metric is invariant under x^+ shifts. The conjugate momentum p^- is conserved. This leads in particular to the absence of spontaneous particle creation.
2. the spacetime is flat except on the $x^- = 0$ plane. The Feynman rules are simplified by using the flat-space coordinates.

We start by canonically quantizing the quadratic part of the lagrangian. The scalar field modes are found by solving the equations of motion (EOM) in the shock wave background with the plane wave conditions in the asymptotic past $x^- < 0$:⁶

$$\begin{aligned} \phi_{p^-, \mathbf{p}}^{\text{in}}(x) &= \theta(-x^-) e^{i[p] \cdot x} + \theta(x^-) \int \frac{d^2 \mathbf{q}}{(2\pi)^2} I(p^-, \mathbf{q}) e^{i[p+\mathbf{q}] \cdot x}, \\ I(p^-, \mathbf{q}) &\equiv \int d^2 \mathbf{x} e^{-i\mathbf{q} \cdot \mathbf{x}} e^{i\frac{1}{2} p^- \Phi(\mathbf{x})}. \end{aligned} \quad (4.2)$$

The compact ‘‘vector in square brackets’’ notation denotes an on-shell 4-vector whose $+$ component is computed in terms of the known $-$ and \perp , i.e. $[p + \mathbf{q}] \equiv ((\mathbf{p} + \mathbf{q})^2 / p^-, p^-, \mathbf{p} + \mathbf{q})$, etc.

⁶By boldface letters \mathbf{p}, \mathbf{x} we denote the 2-dimensional, transverse to the beam, part of 4-dimensional Lorentz vectors. The Minkowski space signature is $-+++$.

The function $I(p^-, \mathbf{q})$ is identical to the eikonal amplitude (2.3), up to the normalization and the absence of -1 under the integral sign (which means that it contains an extra δ -function piece).

The modes (4.2) solve the Klein-Gordon equation both for $x^- < 0$ and for $x^- > 0$. Across the shock wave, they satisfy the matching condition of Section 2.2:

$$\phi(x^- = +\varepsilon, x^+, \mathbf{x}) = \phi(x^- = -\varepsilon, x^+ - \Phi(\mathbf{x}), \mathbf{x}).$$

We proceed to quantize the field by expanding in oscillators:

$$\begin{aligned} \phi(x) &= \int_{p^- > 0} \frac{dp^- d^2 \mathbf{p}}{\sqrt{2p^-} (2\pi)^3} \left\{ a_{p^- \mathbf{p}} \phi_{p^- \mathbf{p}}^{\text{in}}(x) + a_{p^- \mathbf{p}}^\dagger [\phi_{p^- \mathbf{p}}^{\text{in}}(x)]^* \right\}, \\ [a_{p_1^- \mathbf{p}_1}, a_{p_2^- \mathbf{p}_2}^\dagger] &= (2\pi)^3 \delta(p_1^- - p_2^-) \delta^{(2)}(\mathbf{p}_1 - \mathbf{p}_2). \end{aligned}$$

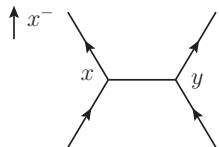
Such normalization of the creation/annihilation operators is standard for quantizing on the light cone; it differs from the usual one by a simple rescaling.

Equivalently, we can quantize using the outgoing modes, which reduce to plane waves for $x^- > 0$:

$$\phi_{p^-, \mathbf{p}}^{\text{out}}(x) = \theta(x^-) e^{i[p \cdot x]} + \theta(-x^-) \int \frac{d^2 \mathbf{q}}{(2\pi)^2} I(p^-, \mathbf{q}) e^{i[p - \mathbf{q}] \cdot x}. \quad (4.3)$$

The in and out modes are related by a unitary Bogoliubov transformation, which acts only on the transverse momentum \mathbf{p} but not on p^- . Thus there is no spontaneous particle creation in this background; the vacuum is unambiguously defined.

Let us now build a perturbation theory for transition amplitudes. The logic is simplest in the position space. Even though the metric is singular at $x^- = 0$, it is easy to see that $\sqrt{g} \equiv 1$: the metric determinant drops out of the interaction lagrangian. Thus the Feynman diagrams will be given by flat space integrals, with no singular contribution from the shock wave. For instance, the t -channel diagram contributing to the $p_1, p_2 \rightarrow p_3, p_4$ transition amplitude will be given by:



$$= (-i\lambda)^2 \int d^4 x d^4 y [\phi_3^{\text{out}}(x)]^* [\phi_4^{\text{out}}(y)]^* G(x, y) \phi_1^{\text{in}}(x) \phi_2^{\text{in}}(y). \quad (4.4)$$

The ϕ^{out} and ϕ^{in} enter as the in and out state wavefunctions. The propagator $G(x, y)$ must be x^- -ordered:

$$G(x, y) = \theta(x^- - y^-) \langle 0 | \phi(x) \phi(y) | 0 \rangle + (x \leftrightarrow y).$$

In (4.4) we have to integrate in all possible x^- orderings of x and y with respect to each other and to the shock wave sitting at $x^- = 0$. The propagator will take different forms depending on the ordering. For x^- and y^- on the same side of the shock, we get the flat space result:

$$G_{\text{flat}}(x, y) = \theta(x^- > y^- > 0) \int_{p^- > 0} \frac{dp^- d^2 \mathbf{p}}{2p^- (2\pi)^3} e^{i[p] \cdot (x-y)} + (x \leftrightarrow y).$$

On the other hand, across the shock wave we have

$$G_{\text{cross}}(x, y) = \theta(x^- > 0 > y^-) \int_{p^- > 0} \frac{dp^- d^2 \mathbf{p}}{2p^- (2\pi)^3} \int \frac{d^2 \mathbf{q}}{(2\pi)^2} I(p^-, \mathbf{q}) e^{i[p+\mathbf{q}] \cdot x - i[p] \cdot y} + (x \leftrightarrow y).$$

The momentum-space Feynman rule can now be found by straightforward Fourier transformation; they are as follows. The in and out states are specified by the p^- and \mathbf{p} of all incoming and outgoing particles. The transition amplitude $i \rightarrow f$ in the external gravitational field of particle A is then given by:

$$\text{out} \langle f|i \rangle_{\text{in}} = 2(2\pi) \delta(p_f^- - p_i^-) \mathcal{M}(i \rightarrow f).$$

The $\mathcal{M}(i \rightarrow f)$ is a function of the external momenta computed as a series in λ according to the following rules. To obtain the $O(\lambda^N)$ term:

- Draw the Feynman diagrams with N ϕ^3 vertices, considering all possible x^- -orderings of these vertices with respect to each other and to the shock wave at $x^- = 0$.
- Consider all shock wave crossings as additional vertices, with entering transverse momenta \mathbf{q}_a representing momentum exchange with the shock wave.
- Assign p^-, \mathbf{p} internal lines momenta by using their conservation in all vertices (ϕ^3 and shock wave crossings). Momentum flow is in the direction of increasing x^- . The internal p^+ momenta are not conserved but are assigned by using the on-shell condition $p^+ = \mathbf{p}^2/p^-$.
- For each ϕ^3 vertex multiply by $-i\lambda$.
- For each shock wave crossing vertex multiply by $p^- I(p^-, \mathbf{q}_a)$, where p^- is conserved in the crossing.
- For each internal line (i.e. a line connecting two vertices, ϕ^3 or shock wave crossing) carrying momentum p^- , multiply by $\theta(p^-)/p^-$.

- The ϕ^3 vertices and the shock wave at $x^- = 0$ divide the x^- axis into two unbounded and N bounded intervals. For each bounded interval, we define an *intermediate state*, consisting of all the particles whose internal lines traverse this interval. For each intermediate state at *negative* x^- , the amplitude is multiplied by

$$\frac{i}{\sum_i p^+ - \sum_{\text{interm}} p^+ + i\varepsilon}.$$

For each intermediate state at *positive* x^- , it is multiplied by

$$\frac{i}{\sum_f p^+ - \sum_{\text{interm}} p^+ + i\varepsilon}.$$

The sums are over all particles in the initial ($x^- = -\infty$), intermediate, and final ($x^- = +\infty$) state.

- Integrate over the momenta \mathbf{q}_a exchanged with the shock wave:

$$\int (2\pi)^2 \delta^{(2)}(\sum \mathbf{q}_a + \mathbf{p}_i - \mathbf{p}_f) \prod \frac{d^2 \mathbf{q}_a}{(2\pi)^2}.$$

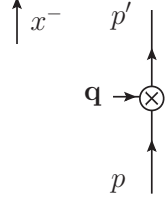
- For loop diagrams, integrate over all undetermined momenta (k^-, \mathbf{k}):

$$\int \frac{dk^- d^2 \mathbf{k}}{2(2\pi)^3}.$$

The reader will notice a striking similarity to the usual light-cone perturbation theory (PT) rules [30]. Notice in particular the light-cone energy denominators, and the $\theta(p^-)$ factors, which eliminate some of the diagrams present in the time-ordered ‘old’ perturbation theory. New features in our case are the shock wave crossing vertices, and that there are two types of energy denominators, depending on the ordering with respect to the shock wave. We thus have ‘light-cone PT in presence of an instantaneous interaction’. Many years ago, Bjorken, Kogut and Soper [31] have developed light-cone PT in external electromagnetic field, and argued that at sufficiently high energies interaction with the external field can be represented as an instantaneous eikonal scattering.⁷ In our case, the eikonal factor has gravitational origin, but the formalism is the same. The formalism of [31] has found application in the dipole scattering approach to the DIS at small x : an almost-real photon splits into two quarks which then undergo eikonal scattering in the gluon field of the proton [32]. The difference is that the gluon field of the proton is not really known, while in our case the eikonal phase can be computed exactly.

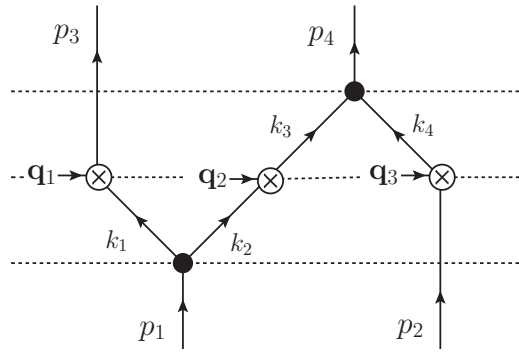
⁷We thank Zoltan Kunszt for bringing this work to our attention.

We will now demonstrate the rules by computing a couple of amplitudes. The elastic one-particle amplitude $\mathcal{M}(p \rightarrow p')$ is given by just one diagram with a shock wave crossing vertex (denoted by a cross):



$$\mathcal{M}(p \rightarrow p') = p^- I(p^-, \mathbf{p} - \mathbf{p}') \quad (p^2 = p'^2 = 0, p^- = p'^-) . \quad (4.5)$$

As a more complicated example, let us compute one of the diagrams appearing in the computation of the amplitude $p_1, p_2 \rightarrow p_3, p_4$:⁸



We have two ϕ^3 vertices and three shock wave crossings. The dotted lines stress the x^- ordering of the vertices. The k_i are the internal line momenta, whose $-$ and \perp components are fixed via momentum conservation, while the $+$ components are determined by being on shell. There are two intermediate states: one before the shock wave (k_1, k_2, p_2) , and one after (p_3, k_3, k_4) . The value of this diagram is thus:

$$\begin{aligned} & \int (2\pi)^2 \delta^{(2)}(\sum \mathbf{q}_a + \mathbf{p}_1 + \mathbf{p}_2 - \mathbf{p}_3 - \mathbf{p}_4) \prod_{a=1}^3 \frac{d^2 \mathbf{q}_a}{(2\pi)^2} \\ & \times (-i\lambda)^2 k_1^- I(k_1^-, \mathbf{q}_1) k_2^- I(k_2^-, \mathbf{q}_2) p_2^- I(p_2^-, \mathbf{q}_1) \\ & \times \frac{i}{(p_1^+ + p_2^+) - (k_1^+ + k_2^+ + p_2^+) + i\varepsilon} \frac{i}{(p_3^+ + p_4^+) - (p_3^+ + k_3^+ + k_4^+) + i\varepsilon} \prod_{i=1}^4 \frac{\theta(k_i^-)}{k_i^-} . \end{aligned}$$

⁸In physical applications below we will be computing amplitudes with one incoming and several outgoing particles. This amplitude containing two incoming particles is considered for illustrative purposes only.

Finally, we have to discuss the relation between the transition amplitude $\mathcal{M}(i \rightarrow f)$ and the full relativistic scattering amplitude \mathcal{M}_{rel} , i.e. the one obtained when we reinstate particle A as a quantum particle as opposed to replacing it with its classical field. We have:

$$\mathcal{M}_{\text{rel}}(A + i \rightarrow A' + f) = -i 2p_A^+ \mathcal{M}(i \rightarrow f). \quad (4.6)$$

The incoming (outgoing) momenta of particle A are assigned as follows:

$$p_A = (p_A^+, 0, 0), \quad p'_A = (p_A^+, 0, \mathbf{p}_i - \mathbf{p}_f).$$

In other words, particle A absorbs the total transverse momentum exchanged with the shock wave. As long as the momentum transfer is small compared to p_A^+ , A' is almost on shell and the approximation is justified.

The relative factor $-i 2p_A^+$ in (4.6) is related to the normalization of the particle A state, which is lost when we replace it with a classical field. This factor is thus process-independent. For instance one can extract it from the external field approximation in QED [24]. The extra i can be traced back to the external field creation vertex, which carries a factor of i .

This settles the question of relativistic normalization of the amplitudes computed via 't Hooft's method. We can now complete the comparison with the resummation method. Using Eqs. (4.5), (4.6) we have

$$\mathcal{M}_{\text{rel}}(A + B \rightarrow A' + B') = -2ip_A^+ p_B^- I(p_B^-, \mathbf{q}), \quad (4.7)$$

which agrees with the eikonal amplitude from Eq. (2.2) including the normalization, modulo the difference between the S- and T-matrices already discussed in Section 2.2.

4.2 Gauge field

In order to keep technical details to a minimum, we will not consider fermionic fields in the shock wave background. Instead, we will stick to a toy model in which charged matter (partonic constituents of the colliding hadrons) consists of massless scalars. This will be sufficient given our general goals. On the other hand, since the coupling constant of the ϕ^3 lagrangian has dimension of mass, the cubic self-interaction is not a good model for the QCD radiation. We do have to introduce gauge fields. Thus we switch from (4.1) to a different microscopic lagrangian, describing the SU(3) Yang-Mills theory and a massless complex scalar in the fundamental representation, propagating in the shock wave background:

$$\mathcal{L} = \sqrt{g} \left(\frac{1}{2} g^{\mu\nu} (D_\mu \phi)^* D_\nu \phi - \frac{1}{2} \text{Tr}[F^{\mu\nu} F_{\lambda\sigma}] \right). \quad (4.8)$$

Most of the ϕ^3 formalism is carried over with trivial changes. Instead of repeating the whole discussion, we will introduce the necessary modifications on a concrete example.

Namely, let us consider the one-gluon emission: particle B , while scattering in the gravitational field of particle A , emits a gluon. The amplitude is given by the sum of the following two diagrams:

(I)
(II)

(4.9)

The new objects are the gluon emission and the gluon shock wave crossing vertices.

To simplify the computations, we will impose the Lorenz and light-cone gauge conditions:

$$D^\mu A_\mu = 0, \quad A_+ = 0.$$

The treatment in a general gauge and demonstration of gauge invariance is given in Appendix A.

Gluon emission in curved space is described by the cubic term in the lagrangian:

$$ig_s \int d^4x \sqrt{g} g^{\mu\nu} \phi_i^* \overleftrightarrow{\partial}_\mu \phi_j (T^a)_{ij} A_\nu^a. \quad (4.10)$$

Here g_s is the strong coupling constant, and the $SU(3)$ generators are normalized by $\text{Tr}(T^a T^b) = 1/2$. In the light-cone gauge the singular component $g^{++} \propto \delta(x^-)$ drops out (see Appendix A for a more detailed discussion). The gluon emission vertex is thus the same as in flat space:

$$g_s T_{ij}^a (p_1 + p_2) \cdot \epsilon \quad \longrightarrow \quad g_s T_{ij}^a (\mathbf{p}_1 + \mathbf{p}_2 - \frac{p_1^- + p_2^-}{l^-} \mathbf{l}) \cdot \epsilon \quad (\epsilon_+ = 0, l \cdot \epsilon = 0), \quad (4.11)$$

where we used the Lorenz gauge to eliminate the ϵ_- component.

The gluon shock wave crossing vertex contains the same factor $p^- I(p^-, \mathbf{q})$ as in the scalar case. A new feature is that the ϵ_- polarization component changes in the crossing according to:

$$\epsilon_{2-} = \epsilon_{1-} - \frac{\boldsymbol{\epsilon}_1 \cdot \mathbf{q}}{p_1^-}, \quad \epsilon_2 = \epsilon_1 \quad (\epsilon_+ \equiv 0), \quad (4.12)$$

This rule is easy to guess from consistency with the imposed gauge; see Appendix A for an explicit derivation. Notice however that we don't have to keep track of this change in ε_- if we use the simplified gluon emission vertex in (4.11).

We are now ready to evaluate the above two diagrams. Working for simplicity in the frame where $\mathbf{p} = 0$, we get:

$$\begin{aligned} \mathcal{M}^{(I)} &= ig_s T_{ij}^a I(p^-, \mathbf{q}) \frac{(2\mathbf{p}' + \mathbf{1} - \frac{2p'^- + l^-}{l^-} \mathbf{1}) \cdot \boldsymbol{\varepsilon}}{p'^+ + l^+ - [p' + l]^+}, \\ \mathcal{M}^{(II)} &= ig_s T_{ij}^a \int \frac{d^2 \mathbf{k}}{(2\pi)^2} I(l^-, \mathbf{k}) I(p'^-, \mathbf{q} - \mathbf{k}) \frac{(\mathbf{k} - \mathbf{1} - \frac{2p^- - l^-}{l^-} (\mathbf{1} - \mathbf{k})) \cdot \boldsymbol{\varepsilon}}{-[p - l + \mathbf{k}]^+ - [l - \mathbf{k}]^+ + i\varepsilon}. \end{aligned} \quad (4.13)$$

Physical consequences of the derived expressions will be discussed below.

As a final comment, we note that lagrangian (4.8) contains also a cubic gluon self-interaction vertex, which could be discussed analogously to (4.11), as well as two quartic vertices ($\phi\phi AA$ and $AAAA$). The quartic vertices do not contribute to the amplitudes in the collinearly enhanced region, and we will not need their precise expressions.

5 Initial state radiation in T-scattering

The dominant QCD radiation effects in the usual perturbative hard scattering processes are the collinear initial and final state radiation. We now proceed to see how these effects manifest themselves in the T-scattering. We will focus on the initial state radiation and its effect on the parton distribution scale. Final state radiation, which happens after the partons cross the shock wave, is expected to be as usual.

5.1 Observable

To discuss radiative corrections to the PDFs, we need to choose a process and an observable which can be defined and computed beyond LO. The simplest such process is the T-scattering analogue of the DIS. In other words, we will consider an electron-proton T-scattering $ep \rightarrow e + \text{anything}$ at a fixed momentum transfer. This is like in Fig. 1 with an electron instead of a neutrino.

The scattering is characterized by $t = -q^2$ and q^+ , the energy transfer to the proton. These can be measured by observing the electron. As usual, we assume small angle scattering: $|t| \ll s$. We will also assume that the relative electron energy loss is small, $q^+ \ll p_A^+$. Under these conditions, and also since the electron does not QCD-radiates, we can represent it by a classical relativistic

point particle of fixed energy. This is our ‘particle A ’. Using the A' on shell condition $(p_A - q)^2 = 0$, it is easy to show that the momentum transfer is mostly in the transverse plane, as expressed by the relation:

$$\mathbf{q}^2 = q^2 (1 + 2q^+/p_A^+) \simeq q^2.$$

Like in the DIS, we are interested in the differential cross section with respect to \mathbf{q} and the Bjorken x :

$$\frac{d\sigma}{d^2\mathbf{q} dx}, \quad x = \frac{q^2}{p_B^- q^+}, \quad 0 < x < 1.$$

As is customary, we will first analyze the partonic cross section $\hat{\sigma}$ between the electron and a quark (particle B). We will work in a toy model of scalar quarks. At LO (no gluon emission), the amplitude is (4.7) and the partonic cross section is given by

$$\frac{d\hat{\sigma}_{\text{LO}}}{d^2\mathbf{q} dx} = \delta(x - 1) \frac{1}{4\pi^2} |I(p_B^-, \mathbf{q})|^2.$$

5.2 One gluon emission in momentum space

Armed with the formalism from Section 4, we can easily write down the gluon emission amplitudes. At the NLO we have diagrams with real gluon emission, as in Eq. (4.9), as well as virtual corrections to the external legs and the vertices in the elastic amplitude. As usual, the latter diagrams do not have to be computed explicitly, since they only correct the coefficient of $\delta(x - 1)$.⁹ We thus focus on the real emission.

The partonic cross section with one gluon emitted is given by a phase space integral (see Appendix B)

$$\frac{d\hat{\sigma}_{\text{NLO}}}{d^2\mathbf{q} dx} = \frac{1}{16\pi^2 \hat{s}} \int \frac{d^2\mathbf{l}}{2(2\pi)^3} \int_0^1 \frac{dz}{z(1-z)} \delta(x - \mathbf{q}^2/(p_B^- q^+)) |\mathcal{M}_{\text{rel}}|^2, \quad (5.1)$$

$$q^+ = \mathbf{l}^2/l^- + (\mathbf{q} - \mathbf{l})^2/p_{B'}^-.$$

Here \mathcal{M}_{rel} is the relativistic scattering amplitude $A + B \rightarrow A' + B' + g$, related to the transition amplitude in the external field $\mathcal{M}(B \rightarrow B' + g)$ via Eq. (4.6). The amplitude \mathcal{M} is in turn the sum of the two diagrams (4.9), evaluated in Eq. (4.13).

⁹Vertex corrections play a role in cancelling the IR divergence in the cross section corresponding to the emissions of soft gluons at large angles. This cancellation holds for any hard process. Specifically, it will also happen for the T-scattering because soft gluons do not feel the shock wave of particle A. Thus we do not discuss soft gluons in what follows, concentrating on the collinear divergence.

We are using notation from (4.9) with $p \equiv p_B$, $p' \equiv p_{B'}$. The q^+ is the total $+$ momentum of the quark-gluon system after the collision. The z is the p^- momentum fraction carried off by quark B' :

$$p'^- = zp^-, \quad l^- = (1-z)p^-.$$

Let us first analyze which region of the \mathbf{l} plane contributes to the integral (5.1). For which \mathbf{l} is there a z saturating the δ -function? The relevant function (see Fig. 7)

$$X(z) \equiv \mathbf{q}^2 / (p_B^- q^+) \equiv \frac{\mathbf{q}^2}{(|\mathbf{q} - \mathbf{l}|)^2 / z + \mathbf{l}^2 / (1-z)},$$

has a maximum value

$$\max_{0 < z < 1} X(z) = X(z_*) = \frac{\mathbf{q}^2}{(|\mathbf{q} - \mathbf{l}| + |\mathbf{l}|)^2} \quad (z_* = \frac{|\mathbf{q} - \mathbf{l}|}{|\mathbf{q} - \mathbf{l}| + |\mathbf{l}|}).$$

Thus, the integrand of (5.1) is nonzero for \mathbf{l} belonging to the ellipse:

$$|\mathbf{q} - \mathbf{l}| + |\mathbf{l}| < |\mathbf{q}| / \sqrt{x}.$$

In other words, phase space limits the transverse momentum of the emitted gluon to be at most $\mathcal{O}(\mathbf{q})$.

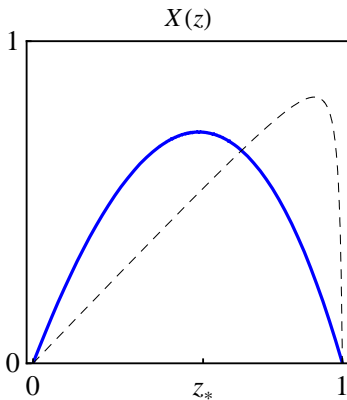


Figure 7: *The function $X(z)$ for a generic \mathbf{l} (solid line) and for $|\mathbf{l}| \ll |\mathbf{q}|$ (dashed line).*

Let us now examine the amplitude, whose two parts are given in Eq. (4.13). By analogy with the usual DIS, we expect that part (I), corresponding to the gluon emission *after* the hard scattering, gives only a finite correction to the cross section, while part (II) contains a logarithmic IR divergence which has to be absorbed by redefining the PDFs. Let us see formally how this happens.

Notice that part (I) of the amplitude is non-singular in the \mathbf{l} plane. In particular, the intermediate state denominator is completely fixed at $\mathbf{q}^2(\frac{1}{x} - 1)/p^- > 0$. Omitting the x dependent factors, the amplitude is thus $\mathcal{O}(g_s I \mathbf{q} \cdot \boldsymbol{\varepsilon} / \mathbf{q}^2)$, and its square is $\mathcal{O}(g_s^2 |I|^2 / \mathbf{q}^2)$. After integrating over the ellipse in the \mathbf{l} plane (area $\sim \pi \mathbf{q}^2$), we get a finite contribution to the differential cross section of the relative order $\mathcal{O}(\alpha_s / \pi)$. This is as expected.

Interesting physics is associated with part (II), whose expression can be simplified as follows:

$$\begin{aligned} \mathcal{M}^{(\text{II})} &= -i g_s T_{ij}^a 2p^- z \boldsymbol{\varepsilon} \cdot \mathbf{M}, \\ \mathbf{M}_i &= \int \frac{d^2 \mathbf{k}}{(2\pi)^2} \frac{(\mathbf{k} - \mathbf{l})_i}{(\mathbf{k} - \mathbf{l})^2} I(zp^-, \mathbf{q} - \mathbf{k}) I((1-z)p^-, \mathbf{k}) \\ &\equiv \frac{-\mathbf{l}_i}{\mathbf{l}^2} \tilde{I}(zp^-, \mathbf{q}) + \frac{(\mathbf{q} - \mathbf{l})_i}{(\mathbf{q} - \mathbf{l})^2} \tilde{I}((1-z)p^-, \mathbf{q}) \\ &\quad + \int \frac{d^2 \mathbf{k}}{(2\pi)^2} \frac{(\mathbf{k} - \mathbf{l})_i}{(\mathbf{k} - \mathbf{l})^2} \tilde{I}(zp^-, \mathbf{q} - \mathbf{k}) \tilde{I}((1-z)p^-, \mathbf{k}). \end{aligned} \tag{5.2}$$

$$\tag{5.3}$$

Here we separated the regular part \tilde{I} of the $I(p^-, \mathbf{q})$ from the δ -function piece describing the propagation without scattering:

$$\begin{aligned} I(p^-, \mathbf{q}) &= (2\pi)^2 \delta^{(2)}(\mathbf{q}) + \tilde{I}(p^-, \mathbf{q}), \\ \tilde{I}(p^-, \mathbf{q}) &= 2\pi b_c^2 F_n(b_c |\mathbf{q}|), \end{aligned}$$

where $F_n(y)$ are the same functions as in Eq. (2.4). We omitted a total $\delta^{(2)}(\mathbf{q})$ piece from (5.3).

The physical meaning of the decomposition (5.3) is as follows. In the first two terms, only one of the two splitting products of quark B participates in the gravitational interaction, the other one passing the shock wave without scattering. The last term instead describes their coherent gravitational scattering, as in Fig. 3. We call it the *rescattering* term, since it corresponds to the situation when the emitted QCD radiation changes its direction in the field of the shock wave.

We now proceed to studying corrections to the cross section. Consider first the case $|\mathbf{q}| \lesssim b_c^{-1}$. In this case all the entering \tilde{I} functions are $\mathcal{O}(2\pi b_c^2)$. The rescattering term can be estimated by integrating up to $|\mathbf{k}| \sim b_c^{-1}$ beyond which point the \tilde{I} decrease faster than $|\mathbf{k}|^{-1}$, and the integral converges. We get

$$|\mathbf{M}_{\text{resc}}| \sim \frac{\pi b_c^{-2}}{(2\pi)^2} b_c (2\pi b_c^2)^2 \sim b_c (2\pi b_c^2) < \frac{1}{|\mathbf{q}|} (2\pi b_c^2) \quad (|\mathbf{q}| \lesssim b_c^{-1}). \tag{5.4}$$

We see that rescattering is subleading to the first two terms in (5.3).

Concentrating on the first two terms, the dominant contribution to the cross section comes from the singularities at $\mathbf{l} \rightarrow 0$ and $\mathbf{l} \rightarrow \mathbf{q}$. Squaring the amplitude and integrating we get:

$$\frac{d\hat{\sigma}_{\text{NLO}}}{d^2\mathbf{q} dx} \simeq \frac{1}{4\pi^2} \left\{ |\tilde{I}(xp^-, \mathbf{q})|^2 P_{Q \rightarrow Q}(x) + |\tilde{I}(xp^-, \mathbf{q})|^2 P_{Q \rightarrow g}(x) \right\} \frac{\alpha_s}{2\pi} \log \frac{\mathbf{q}^2}{\mu_{\text{IR}}^2} \quad (|\mathbf{q}| \lesssim b_c^{-1}),$$

$$P_{Q \rightarrow Q}(x) = C_F \frac{2x}{1-x}, \quad P_{Q \rightarrow g}(x) = P_{Q \rightarrow Q}(1-x), \quad C_F = 4/3. \quad (5.5)$$

Here we used that in the relevant regions of integration (see Fig. 7)

$$x = X(z) \simeq z \quad (|\mathbf{l}| \ll |\mathbf{q}|), \quad x = X(z) \simeq 1-z \quad (|\mathbf{q}-\mathbf{l}| \ll |\mathbf{q}|).$$

Eq. (5.5) has the standard factorized form expected from an NLO QCD correction to a hard scattering [27]. The IR divergent logarithm multiplies the quark-electron and gluon-electron LO cross sections, with the *scalar* quark DGLAP splitting functions $P_{Q \rightarrow Q}$ and $P_{Q \rightarrow g}$ as coefficients¹⁰. As usual, we can absorb the IR divergence into the quark (first term) and gluon (second term) PDFs. If we fix the parton distribution scale at the upper cutoff, $\mu_F^2 = \mathbf{q}^2$, then the whole logarithmic correction is absorbed.

It is of course not surprising that we managed to recover the standard factorization for $|\mathbf{q}| \lesssim b_c^{-1}$: rescattering was not important in this case, and without rescattering there is no difference between transplanckian and any other hard scattering.

Let us proceed to the case $|\mathbf{q}| \gg b_c^{-1}$. The situation here is more complicated since the rescattering is no longer subleading. Consider for example the region $|\mathbf{q}| \gg |\mathbf{l}| \gg b_c^{-1}$. The rescattering integral is dominated by $|\mathbf{k}| \lesssim b_c^{-1}$, where $\tilde{I}((1-z)p^-, \mathbf{k})$ is maximal, and not, say, by the region of $|\mathbf{k}| \sim |\mathbf{l}|$, where $\frac{(\mathbf{k}-\mathbf{l})_i}{(\mathbf{k}-\mathbf{l})^2}$ is maximal. The reason is that $\tilde{I}((1-z)p^-, \mathbf{k})$ decreases faster than $|\mathbf{k}|^{-1}$ for $|\mathbf{k}| \gg b_c^{-1}$. We get an estimate:

$$|\mathbf{M}_{\text{resc}}| \sim \frac{\pi b_c^{-2}}{(2\pi)^2} \frac{1}{|\mathbf{l}|} (2\pi b_c^2) |\tilde{I}(zp^-, \mathbf{q})| \sim \frac{1}{|\mathbf{l}|} |\tilde{I}(zp^-, \mathbf{q})| \quad (|\mathbf{q}| \gg |\mathbf{l}| \gg b_c^{-1}), \quad (5.6)$$

which is comparable to the first term without rescattering in (5.3).

5.3 Impact parameter picture

In a situation when rescattering cannot be neglected, the separation into three terms in Eq. (5.3) becomes artificial, and we should treat the whole amplitude as given in (5.2). Substituting the definitions of I , we can transform this expression into a transverse plane integral:

$$\mathbf{M}_i = \frac{i}{2\pi} \int d^2\mathbf{y}' d^2\mathbf{y} \frac{(\mathbf{y}' - \mathbf{y})_i}{|\mathbf{y}' - \mathbf{y}|^2} e^{-i(\mathbf{q}-\mathbf{l}) \cdot \mathbf{y}' + iz \frac{p^-}{2} \Phi(\mathbf{y}')} e^{-i\mathbf{l} \cdot \mathbf{y} + i(1-z) \frac{p^-}{2} \Phi(\mathbf{y})}. \quad (5.7)$$

¹⁰See [33] for the splitting functions of a colored scalar.

This simple equation provides a key insight into the physics of the process. Namely, we can view the factor $\Psi(\mathbf{y}', \mathbf{y}) = \frac{(\mathbf{y}' - \mathbf{y})_i}{|\mathbf{y}' - \mathbf{y}|^2}$ as the coordinate-space wavefunction of the gluon-quark state into which quark B splits. Upon crossing the shock wave, this two-particle wavefunction is multiplied by the eikonal factors $e^{iz\frac{p^-}{2}\Phi(\mathbf{y}'')}$ and $e^{i(1-z)\frac{p^-}{2}\Phi(\mathbf{y})}$, depending on the transverse plane position of each particle. Finally, to compute the S-matrix element, one takes the overlap with the outgoing state wavefunction $e^{-i(\mathbf{q}-\mathbf{l})\cdot\mathbf{y}'}e^{-i\mathbf{l}\cdot\mathbf{y}}$.¹¹

The completely general expression (5.7) can be further simplified if $|\mathbf{l}| \ll |\mathbf{q}|$. In this case, the typical \mathbf{y} contributing to the integral are much larger than the typical \mathbf{y}' . Approximating $\mathbf{y}' - \mathbf{y} \simeq -\mathbf{y}$, the amplitude takes a factorized form:

$$\mathbf{M}_i \simeq I(zp^-, q) \mathbf{f}_i \quad (|\mathbf{l}| \ll |\mathbf{q}|), \quad (5.8)$$

where the gluon emission factor \mathbf{f}_i is given by

$$\mathbf{f}_i = -\frac{i}{2\pi} \int d^2\mathbf{y} \frac{\mathbf{y}_i}{|\mathbf{y}|^2} e^{-i\mathbf{l}\cdot\mathbf{y} + i(1-z)\left(\frac{b_c}{|\mathbf{y}|}\right)^n} = -\frac{\mathbf{l}_i}{\mathbf{l}^2} \times C_n[(1-z)^{1/n} b_c |\mathbf{l}|], \quad (5.9)$$

$$C_n(u) \equiv \int_0^\infty dy J_1(y) e^{i\left(\frac{u}{y}\right)^n}.$$

This factor has a nontrivial dependence on \mathbf{l} . For $|\mathbf{l}| \ll b_c^{-1}$ the integral is dominated by large $|\mathbf{y}| \gg b_c^{-1}$, so that the second term in the exponent can be dropped, giving

$$\mathbf{f}_i \simeq -\mathbf{l}_i/\mathbf{l}^2 \quad (|\mathbf{l}| \ll b_c^{-1}).$$

Thus we recover the first term in Eq. (5.3), which in this limit dominates the amplitude.

On the other hand, in the opposite limit the integral can be evaluated by stationary phase, with the result:

$$\mathbf{f}_i \simeq \frac{e^{i \times \text{phase}}}{\sqrt{n+1}} \mathbf{l}_i/\mathbf{l}^2 \quad (|\mathbf{l}| \gg b_c^{-1}). \quad (5.10)$$

Remember that precisely in this case we expected a non-negligible contribution from rescattering, see Eq. (5.6). We now see that its effect is indeed important: rescattering leads to an $\mathcal{O}(1)$ reduction of the gluon emission amplitude! Physically, this can be explained as follows. To scatter with large \mathbf{l} , the emitted gluon must cross the shock wave in the region of small impact parameters. In this region, the eikonal factor in (5.9) distorts the gluon wavefunction, which leads to suppression of the amplitude via destructive interference. It is however remarkable that, up to an \mathbf{l} -dependent phase, the suppressed amplitude still goes as $\mathbf{l}_i/\mathbf{l}^2$.

¹¹See [34] where similar considerations are made for a gluon splitting into a $q\bar{q}$ pair in the field of an incoming nucleus.

In terms of the function C_n , the above asymptotics can be stated as follows:

$$C_n(u) \rightarrow 1 \quad (u \rightarrow 0), \quad |C_n(u)| \simeq 1/\sqrt{n+1} \quad (u \gg 1).$$

As can be seen from Fig. 8, the large u behavior sets in already for $u \gtrsim 2$.

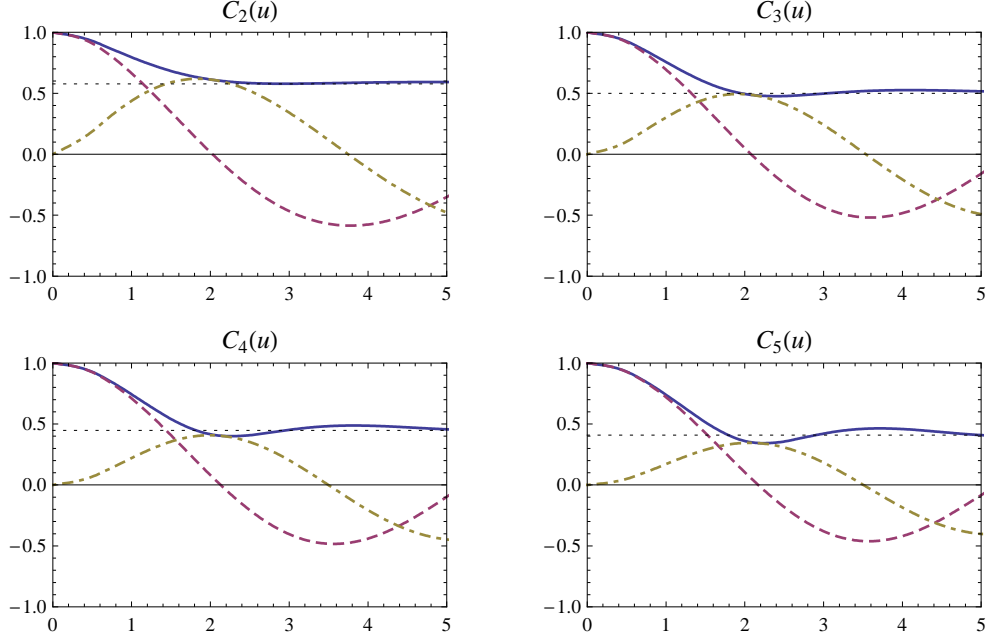


Figure 8: Numerical plots of $C_n(u)$ for $n = 2, 3, 4, 5$: the absolute value (solid blue curve), the real and imaginary parts (dashed and dot-dashed curves), the $u = \infty$ asymptotic value $1/\sqrt{n+1}$ (dotted line).

We are now ready to derive the logarithmic correction to the cross section for $|\mathbf{q}| \gg b_c^{-1}$. We square Eq. (5.8) and integrate in $|\mathbf{l}| \ll |\mathbf{q}|$, taking into account the suppression for $|\mathbf{l}| \gg b_c^{-1}$. Schematically, we get:

$$\int_{|\mathbf{l}| \lesssim |\mathbf{q}|} d^2 \mathbf{l} |\mathbf{f}|^2 \quad \longrightarrow \quad \int_{\mu_{\text{IR}}}^{b_c^{-1}} \frac{dl}{l} + \frac{1}{n+1} \int_{b_c^{-1}}^{|\mathbf{q}|} \frac{dl}{l} = \log \frac{\mu_F(|\mathbf{q}|)}{\mu_{\text{IR}}}. \quad (5.11)$$

In other words, due to the $1/(n+1)$ suppression of the second term, the arguments of the two logs combine into a geometric mean which coincides exactly with Eq. (1.1)!

The final result is as follows: for $|\mathbf{q}| \gg b_c^{-1}$, the NLO correction to the cross section is given by the same Eq. (5.5) as for $|\mathbf{q}| \lesssim b_c^{-1}$ with the following simple replacement:

$$\log \frac{\mathbf{q}^2}{\mu_{\text{IR}}^2} \quad (|\mathbf{q}| \lesssim b_c^{-1}) \quad \longrightarrow \quad \log \frac{\mu_F^2(|\mathbf{q}|)}{\mu_{\text{IR}}^2} \quad (|\mathbf{q}| \gg b_c^{-1}).$$

5.4 Discussion

Let us discuss what we have achieved. First, we have shown that the emission amplitude of near-collinear gluons has a factorized form, Eq. (5.8). Physically, it means that we can first consider the hard scattering process, and worry about adding additional gluons later. If a parton splits in two before crossing the shock wave, one and only one of the splitting products absorbs most of the momentum transfer in a typical event. This is actually an important check of validity of the partonic picture.

Second, we found explicitly the gluon emission factor \mathbf{f}_i . The probability distribution of emitted gluons is given by $|\mathbf{f}_i|^2$. We found that for large relative transverse momenta $|\mathbf{l}| \gg b_c^{-1}$ (but still $|\mathbf{l}| \ll |\mathbf{q}|$) this distribution is suppressed by a factor $1/(n+1)$ relative to the standard QCD distribution $1/\mathbf{l}^2$. This is a new effect, which could be used to measure the number of extra dimensions.

Finally, as a consequence of this suppression, the logarithmic NLO correction to the partonic cross section involves, for $|\mathbf{q}| \gg b_c^{-1}$, a scale which interpolates between the usual $|\mathbf{q}|$ and b_c^{-1} in agreement with Eq. (1.1). In fact, as we show in Appendix C, such logarithms occur in every order of perturbation theory. Thus, as usual, they can be exponentiated and removed by shifting the parton distribution scale to $\mu_F(|\mathbf{q}|)$. This, then, provides a formal justification for the proposal of Emparan, Masip, and Rattazzi [17], that this scale is the one minimizing higher-order corrections.

Our derivation of the scale (1.1) has an added advantage that we now know the gluon distribution. This distribution could not be easily guessed: for example the standard $1/\mathbf{q}^2$ with a sharp b_*^{-1} cutoff would give rise to the same log. At the same time, the very fact that we found agreement with Ref. [17] may seem like a mystery. Remember that they *fixed* this scale to be equal to b_*^{-1} (see Section 3). Where, then, does the typical impact parameter b_* hide in our computation?

In fact, if we are not interested in the gluon distribution, we can reformulate our derivation so that it will conform with the original intuition of [17]. The idea is to compute the LHS of Eq. (5.11) not from the asymptotics of C_n but directly from the definition of \mathbf{f}_i in the impact parameter representation. Since the L_2 norm of the gluon wavefunction is the same in the momentum and in the position space, we have

$$\int_{\mu_{\text{IR}}}^{|\mathbf{q}|} \frac{d^2\mathbf{l}}{(2\pi)^2} |\mathbf{f}|^2 \sim \int d^2\mathbf{y} \left| \frac{\mathbf{y}_i}{|\mathbf{y}|^2} e^{i(1-z)(\frac{b_c}{|\mathbf{y}|})^n} \right|^2 = \int \frac{d^2\mathbf{y}}{\mathbf{y}^2} \propto \log \frac{y_{\text{max}}}{y_{\text{min}}}.$$

The only subtlety is that in the LHS we are not integrating over the whole \mathbf{l} plane, and thus the limits of the \mathbf{y} integration have to be adjusted accordingly. A moment's thought shows that the

correct limits should be put at the typical \mathbf{y} values contributing to \mathbf{f}_i at $|\mathbf{l}| \sim \mu_{\text{IR}}$ and $|\mathbf{l}| \sim |\mathbf{q}|$:

$$y_{\text{max}} \sim \mu_{\text{IR}}^{-1}, \quad y_{\text{max}} \sim b_*.$$

So, we recover the same logarithm as above, and this time b_* enters explicitly.

We have worked throughout in the toy model of scalar quarks. However, it should be easy to adapt our considerations to the realistic case of fermionic matter. One would have to compute the shock wave crossing vertex for the fermion field. This will require solving the Dirac equation in the shock wave background. We expect that our results about factorization and suppression of radiation at large angles will remain true in the fermionic case as well.

6 Simultaneous radiation

So far we were making the technical simplifying assumption that particle A does not QCD-radiate. This is of course not true in pp collisions at the LHC, when both colliding partons are colored. We will now discuss how one could relax or remove this restriction.

Consider the following two key properties of QCD radiation:

1. Near-collinear emission dominates.
2. Its amplitude takes a factorized form.

These properties are true for the standard hard perturbative processes. For the T-scattering with non-radiating A , we have also shown them to be true, provided that a gluon emission factor is adjusted accordingly. We conjecture that these properties continue to hold when both A and B are allowed to radiate. In practice, this implies that the dominant part of the emitted radiation can be described using the independent emission approximation: first compute the radiation off B (taking A classical), then off A (taking B classical).

Intuitively, this can be justified as follows. The fact that the near-collinear emission dominates is due to the $\sim 1/|\mathbf{l}|$ singularity in the gluon emission factor, combined with a phase space cutoff $|\mathbf{l}| \lesssim |\mathbf{q}|$. We have seen that shock wave crossing tends only to suppress radiation at large angles by distorting the gluon wavefunction, and we do not expect this tendency to reverse when A is allowed to radiate. Thus collinear radiation should dominate also for the T-scattering. Once we know that collinear emission dominates, and thus the emitted radiation does not change the hard transverse momentum flow of the process, it seems reasonable that the amplitude should factorize

into the product of the $2 \rightarrow 2$ scattering with the hardest momentum exchange times the gluon emission factors.¹²

The independent emission approximation is probably adequate for most practical purposes. Nevertheless, to try to go beyond it is an interesting theoretical challenge. We will now describe pictorially a generalization of our formalism which, we believe, can describe simultaneous emissions from A and B without any extra approximation (except, of course, large CM energy and small scattering angle).

The starting point is the emission amplitude in the impact parameter representation (5.7) (see Appendix C for its generalizations to two and more gluons). The physical meaning of this equation in terms of the two-particle wavefunction and individual eikonal factors was explained above. Suppose now that both particles split. The amplitude can be constructed according to the following three steps (see Fig. 9).

1. We evolve the partons from infinity to the transverse plane $x^- = x^+ = 0$ where the collision is assumed to happen. We introduce many-particle wavefunctions for the splitting products of both A and B . The total wavefunction in the transverse collision plane is the product of the two:

$$\Psi_{tot} = \Psi_A(\{\mathbf{x}_a\})\Psi_B(\{\mathbf{y}_b\}).$$

Here \mathbf{x}_a (\mathbf{y}_b) are the transverse coordinates of left- and right-movers. The $\Psi_{A,B}$ can be computed via the flat-space light cone perturbation theory. For the one-gluon emission they are the same as in (5.7).

2. When the splitting products cross the transverse collision plane, the wavefunction Ψ_{tot} is multiplied with eikonal factors, one for each pair of opposite-movers. It is not difficult to guess that these factors are equal to

$$\exp iz_a z_b \chi(\mathbf{x}_a - \mathbf{y}_b),$$

where χ is the $2 \rightarrow 2$ eikonal phase from (2.3), and $z_a = p_a^+/p_A^+$, $z_b = p_b^-/p_B^-$ are the longitudinal momentum fractions carried by partons a and b .

¹²We are ignoring here soft gluons which may be exchanged between particles A and B. In case of standard hard QCD processes involving two initial hadrons, like in Drell-Yan, where proofs of factorization to all orders in perturbation theory exist [35], it is known that such soft gluon exchanges cancel in the total cross section. We expect this cancellation to carry over to our case, because soft gluons do not feel the gravitational field of the energetic particles (the eikonal factor being proportional to the gluon energy).

3. Finally, to find S-matrix elements, we compute the overlap with the outgoing state wavefunctions. These are simple plane waves if the partons do not undergo any splittings after the shock wave crossings. If such splittings are present, like in part (I) of (4.9), these are more complicated functions of external momenta. However, since at this stage left- and right-movers no longer interact, the flat-space light cone perturbation theory can be used to find them.

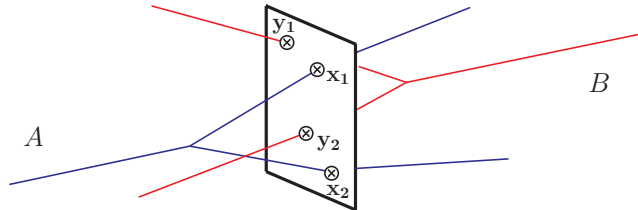


Figure 9: *This diagram represents one of the terms in the amplitude $A + B \rightarrow A' + g + B' + g$, in which both the right-moving A and left-moving B split before colliding.*

We think that this generalized formalism, apart from providing an attractive mental picture, could find interesting future applications, especially in the problem of gravitational radiation emission.

7 Conclusions

The main point of this paper is that including radiation in small-angle transplanckian scattering is, after all, a tractable problem. The gravitational interaction producing eikonal phase factors happens instantaneously, while the processes of particle splitting are spread in time. Based on this observation, we developed a formalism which allows explicit computations of scattering amplitudes in presence of hard, quantum, radiation. In the impact parameter representation, the radiating particle splits into a multi-particle virtual state, whose wavefunction, computed via light-cone perturbation theory, is then multiplied by individual eikonal factors.

We demonstrated the usefulness of our formalism on the concrete problem of initial state QCD radiation in transplanckian scattering. We will not repeat here the detailed discussion of the obtained results given in the Introduction and in Section 5.4. We believe however that this example by no means exhausts the list of possible applications. We are particularly hopeful about

a possibility to shed new light on the problem of gravitational radiation emission, which is always on our mind.

8 Acknowledgements

We thank Babis Anastasiou, Stefano Frixione, Paolo Nason, Carlo Oleari, and especially Zoltan Kunszt and Riccardo Rattazzi for useful discussions and comments. This work is partially supported by the EU under RTN contract MRTN-CT-2004-503369 and by MIUR under the contract PRIN-2006022501. We thank the Galileo Galilei Institute for Theoretical Physics for the hospitality and the INFN for partial support during the completion of this work.

A Gluon field in the shock wave background

Here we will discuss quantization of the free gluon field in the shock wave background, as well as the gluon emission vertices, the gauge invariance, and the absence of gluon emission terms localized on the shock wave.

We start from the Maxwell Lagrangian in curved spacetime, which integrating by parts can be rewritten as

$$\mathcal{L} = -\frac{1}{4}\sqrt{g}F^{\mu\nu}F_{\lambda\sigma} \rightarrow -\frac{1}{2}\sqrt{g}[(D_\mu A_\nu)(D^\mu A^\nu) - (D_\mu A^\mu)^2 + {}^{(4)}R_{\mu\nu}A^\mu A^\nu].$$

Notice that while the D -dimensional Ricci tensor of the AS metric is zero for $x_\perp \neq 0$ as a consequence of Einstein's equation, the 4-dimensional Ricci tensor of the metric $g_{\mu\nu}$ induced on the SM brane is nonzero. Namely, it has a nonzero component

$${}^{(4)}R_{--} = -\frac{1}{2}\delta(x^-)\partial_{\mathbf{x}}^2\Phi \neq 0$$

(compare with (2.6) where the Laplacian is with respect to all $D - 2$ transverse directions).

Let us fix the curved space Lorenz gauge $D_\mu A^\mu = 0$. In this gauge the EOM take the form:

$$D^2 A_\nu - {}^{(4)}R_\nu{}^\mu A_\mu = 0. \tag{A.1}$$

We first discuss the gluon propagator across the shock wave. To find it we need to solve the EOM with the initial conditions $A_\mu = \varepsilon_\mu e^{ipx}$ for $x^- < 0$.

Consider first the light-cone gauge case $\varepsilon_+ = 0$. It is easy to see that the shock wave metric has $\Gamma_{+\nu}^\mu \equiv 0$, which implies $A_+ \equiv 0$. The other gauge field components are found to satisfy the

equations:

$$\begin{aligned}\partial_+ \partial_- \mathbf{A} + \delta(x^-) \Phi(\mathbf{x}) \partial_+^2 \mathbf{A} &= \frac{1}{4} \partial_{\mathbf{x}}^2 \mathbf{A}, \\ \partial_+ \partial_- A_- + \delta(x^-) [\Phi(\mathbf{x}) \partial_+^2 A_- + \frac{1}{2} \partial_i \Phi(\mathbf{x}) \partial_+ \mathbf{A}_i] &= \frac{1}{4} \partial_{\mathbf{x}}^2 A_-, \end{aligned}$$

Just as in the scalar field case, it is enough to find a matching condition, i.e. to relate solution of these equations for $x^- = -\epsilon$ and $x^- = +\epsilon$. One could use the method of Section 2.2 based on transforming to the \tilde{x} coordinates. Here we want to demonstrate a different, equivalent, approach. Namely, we regularize the above equations by smearing the δ -functions. One can show that the terms put in the RHS of the equations can be dropped in this analysis, since their effect goes to zero when the regulator is removed. All the other terms are however important.

From the first equation, we find how the transverse components varies across the shock wave:

$$\mathbf{A} = \epsilon e^{-i\frac{p_-^-}{2}x^+ + i\mathbf{p}\cdot\mathbf{x}} \exp\left(i\frac{p_-^-}{2} \int_{-\epsilon}^{x^-} \delta(x^-) \Phi(\mathbf{x})\right). \quad (\text{A.2})$$

Substituting this solution into the equation for A_- we find:

$$A_- = \left[\epsilon_- - \frac{1}{2}\theta(x^-)\epsilon_i \partial_i \Phi(\mathbf{x})\right] e^{-i\frac{p_-^-}{2}x^+ + i\mathbf{p}\cdot\mathbf{x}} \exp\left(i\frac{p_-^-}{2} \int_{-\epsilon}^{x^-} \delta(x^-) \Phi(\mathbf{x})\right). \quad (\text{A.3})$$

Thus on the other side of the shock wave:

$$\begin{aligned}\mathbf{A}(x^- = +\epsilon) &= \epsilon e^{-i\frac{p_-^-}{2}(x^+ - \Phi(\mathbf{x})) + i\mathbf{p}\cdot\mathbf{x}}, \\ A_-(x^- = +\epsilon) &= \left(\epsilon_- - \frac{1}{2}\epsilon_i \partial_i \Phi(\mathbf{x})\right) e^{-i\frac{p_-^-}{2}(x^+ - \Phi(\mathbf{x})) + i\mathbf{p}\cdot\mathbf{x}}.\end{aligned}$$

These are the desired matching conditions. Taking the Fourier transform we recover the rule (4.12).

A general solution of the EOM (A.1) is a linear combination of the just found solution in the gauge $A_+ = 0$ with a pure gauge solution

$$A_\mu = \partial_\mu \psi. \quad (\text{A.4})$$

The gauge parameter ψ is given by Eq. (4.2) as a general solution to the Klein-Gordon equation.

Let us now discuss the gluon emission term (4.10) in a general gauge. There are several quantities in (4.10) with δ -function singularities on the shock wave. Thus one may wonder if there is a contact emission term localized on the shock wave. In fact such a contribution is absent, so that one can always compute the gluon emission as a sum of two separate integrals for $x^- > 0$ and $x^- < 0$. To see this, one can argue as follows.

First of all, as already mentioned in Section 4.2, localized terms are absent in the light-cone gauge $A_+ = 0$. In this gauge A_μ does not contain δ -function singularities as one can see from the explicit solution (A.2),(A.3). The δ -function does appear in g^{++} and in $\phi^* \overleftarrow{\partial}_- \phi$, but all contractions involving these terms necessarily contain A_+ and vanish.

Second, consider the pure gauge case (A.4). In this case there are several δ -function terms in (4.10). However, one can show that they cancel among themselves. The reason for this cancellation is as follows. Since the integrand in (4.10) is a Lorentz invariant, we can compute it in the \tilde{x} coordinates (2.8). In these coordinates both ϕ and ψ are continuous, and the integrand has at most θ -function singularity on the shock wave.

To demonstrate the absence of localized terms by a concrete example, let us show that the one-gluon emission amplitude is gauge invariant. We thus have to show that the amplitude to emit a longitudinally polarized gluon is zero, without inclusion of any extra terms localized on the shock wave. The one-gluon emission amplitude is given by the coordinate-space integral:

$$\mathcal{M} = i \int d^4x \sqrt{g} g^{\mu\nu} \left\{ [\phi_{p'}^{\text{out}}(x)]^* \overleftarrow{\partial}_\mu \phi_p^{\text{in}}(x) \right\} A_\nu^{\text{out}}(l, \varepsilon; x).$$

Here $A_\nu^{\text{out}}(l, \varepsilon; x)$ is the outgoing gluon wavefunction. In the considered longitudinal case $\varepsilon_\mu = l_\mu$ we have:

$$A_\mu^{\text{out}}(l, \varepsilon; x) \propto \partial_\mu \phi_l^{\text{out}}(x).$$

The integral splits into two parts: $x^- > 0$, $x^- < 0$. Each of these can be integrated by parts and, using the current conservation, reduces to a boundary term localized on the shock wave. These boundary terms are not quite identical:

$$\begin{aligned} \mathcal{M}_{(x^- > 0)} &= - \int dx^+ d^2\mathbf{x} \left\{ e^{i(\frac{1}{2}p'^- x^+ - \mathbf{p}' \cdot \mathbf{x})} \overleftarrow{\partial}_+ e^{-i(\frac{1}{2}p^- [x^+ - \Phi(\mathbf{x})] - \mathbf{p} \cdot \mathbf{x})} \right\} e^{i(\frac{1}{2}l^- x^+ - \mathbf{l} \cdot \mathbf{x})}, \\ \mathcal{M}_{(x^- < 0)} &= \int dx^+ d^2\mathbf{x} \left\{ e^{i(\frac{1}{2}p'^- [x^+ + \Phi(\mathbf{x})] - \mathbf{p}' \cdot \mathbf{x})} \overleftarrow{\partial}_+ e^{-i(\frac{1}{2}p^- x^+ - \mathbf{p} \cdot \mathbf{x})} \right\} e^{i(\frac{1}{2}l^- [x^+ + \Phi(\mathbf{x})] - \mathbf{l} \cdot \mathbf{x})}. \end{aligned}$$

However, after integrating in x^+ and taking into account the resulting p^- -conserving δ -function, they are seen to cancel.

B Light-cone phase space

The partonic cross section with n gluons emitted $A + B \rightarrow A' + B' + g_1 + \dots + g_n$ is given by the phase space integral

$$d\hat{\sigma} = \frac{1}{2\hat{s}} |\mathcal{M}_{\text{rel}}^{(n)}|^2 (2\pi)^4 \delta^{(4)}(p_i - p_f) d\Phi_{(n+2)}.$$

We assume that A and B collide head on along the z direction. We use the light-cone phase space adapted to the direction of motion of each particle:

$$d\Phi_{(n+2)} = \frac{dp_{A'}^+ d^2\mathbf{p}_{A'}}{(2\pi)^3 2p_{A'}^+} \frac{dp_{B'}^- d^2\mathbf{p}_{B'}}{(2\pi)^3 2p_{B'}^-} \prod \frac{dl_i^- d^2\mathbf{l}_i}{(2\pi)^3 2l_i^-},$$

$$\delta^{(4)}(p_i - p_f) = 2\delta(p_i^+ - p_f^+) \delta(p_i^- - p_f^-) \delta^{(2)}(\mathbf{p}_i - \mathbf{p}_f).$$

The momentum conserving δ -function is saturated by integrating in $dp_{A'}^+ d^2\mathbf{p}_{A'} dp_{B'}^-$, which gives

$$d\hat{\sigma} = \frac{1}{16\pi^2 \hat{s}^2} |\mathcal{M}_{\text{rel}}^{(n)}|^2 \frac{p_B^-}{p_{B'}^-} d^2\mathbf{p}_{B'} \prod \frac{dl_i^- d^2\mathbf{l}_i}{(2\pi)^3 2l_i^-}.$$

The differential cross section in the momentum transfer \mathbf{q} and the Bjorken x is thus given by:

$$\frac{d\hat{\sigma}}{d^2\mathbf{q} dx} = \frac{1}{16\pi^2 \hat{s}^2} \int |\mathcal{M}_{\text{rel}}^{(n)}|^2 \frac{p_B^-}{p_{B'}^-} \prod \frac{dl_i^- d^2\mathbf{l}_i}{(2\pi)^3 2l_i^-} \delta\left(x - \frac{\mathbf{q}^2}{p_B^- q^+}\right),$$

where $q^+ = \mathbf{p}_{B'}^2/p_{B'}^- + \sum \mathbf{l}_i^2/l_i^-$, $\mathbf{p}_{B'} = \mathbf{q} - \sum \mathbf{l}_i$, $p_{B'}^- = p_B^- - \sum l_i^-$ under the integral sign.

C Multi-gluon emission

Let us look at the leading logarithmic corrections to the cross section which come from the radiation of many gluons. We want to verify that they have the correct form in order to be reabsorbed into the PDFs normalized at the scale $\mu_F(q)$.

To begin with, consider the emission of two gluons. In the LLA, we are looking for $(\alpha_s \log \frac{\mu_F}{\mu_{\text{IR}}})^2$ corrections to the cross section. One can show that, because of the form of the denominators in our Feynman rules, a gluon which does not cross the shock wave will not give rise to a large logarithm. Thus the relevant diagrams are those with both gluons emitted at $x^- < 0$, shown in Fig. 10. Let us consider the first of these diagrams, and define:

$$\begin{cases} p'^- = z_1 z_2 p^- \\ l_2^- = (1 - z_2) p^- \\ l_1^- = z_2 (1 - z_1) p^- . \end{cases}$$

Computing this amplitude using the Feynman rules and going into the impact parameter repre-

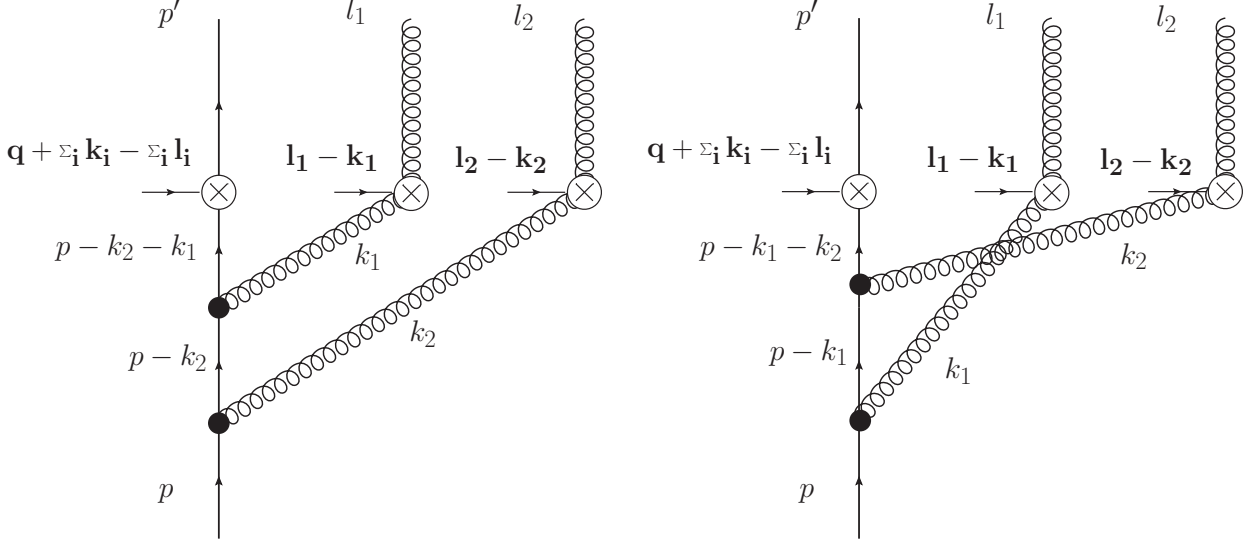


Figure 10: *Relevant diagrams for the emission of 2 gluons.*

sentation, we find $\mathcal{M}^{(l_2 l_1)} = -8p'^-(ig_s)^2 \mathbf{M}_{ij}^{(l_2 l_1)} \boldsymbol{\varepsilon}_{1i} \boldsymbol{\varepsilon}_{2j}$, with:

$$\begin{aligned}
\mathbf{M}_{ij}^{(l_2 l_1)} &= \int \frac{d^2 \mathbf{k}_1}{(2\pi)^2} \frac{d^2 \mathbf{k}_2}{(2\pi)^2} \frac{\mathbf{k}_{2j}}{(\mathbf{k}_2)^2} \frac{(\frac{1}{1-z_1} \mathbf{k}_1 + \mathbf{k}_2)_i}{(\frac{1}{1-z_1} \mathbf{k}_1^2 + \frac{1-z_2+z_1 z_2}{1-z_2} \mathbf{k}_2^2 + 2\mathbf{k}_1 \cdot \mathbf{k}_2)} \\
&\quad \times I(z_1 z_2 p^-, \mathbf{q} + \mathbf{k}_1 + \mathbf{k}_2 - \mathbf{l}_1 - \mathbf{l}_2) I(z_2(1-z_1)p^-, \mathbf{l}_1 - \mathbf{k}_1) I((1-z_2)p^-, \mathbf{l}_2 - \mathbf{k}_2) \\
&\equiv -\frac{1}{(2\pi)^2} \int d^2 \mathbf{x} d^2 \mathbf{y}_1 d^2 \mathbf{y}_2 \frac{(\mathbf{x} - \mathbf{y}_1)_i}{|\mathbf{x} - \mathbf{y}_1|^2} \frac{(\mathbf{x} - \mathbf{y}_2)_j + B(\mathbf{x} - \mathbf{y}_1)_j}{|(\mathbf{x} - \mathbf{y}_2) + B(\mathbf{x} - \mathbf{y}_1)|^2 + A|\mathbf{x} - \mathbf{y}_1|^2} \\
&\quad \times e^{-i(\mathbf{q} - \mathbf{l}_1 - \mathbf{l}_2) \cdot \mathbf{x} + iz_1 z_2 \frac{p^-}{2} \Phi(\mathbf{x})} e^{-i\mathbf{l}_1 \cdot \mathbf{y}_1 + iz_1(1-z_2) \frac{p^-}{2} \Phi(\mathbf{y}_1)} e^{-i\mathbf{l}_2 \cdot \mathbf{y}_2 + i(1-z_2) \frac{p^-}{2} \Phi(\mathbf{y}_2)},
\end{aligned}$$

where $A = z_1(1-z_1)/(1-z_2)$, $B = 1-z_1$. The integrand has the expected form (three-particle wavefunction in the transverse plane) \times (individual eikonal factors) \times (outgoing states).

Let us estimate this amplitude for $|\mathbf{q}| \gg |\mathbf{l}_1|, |\mathbf{l}_2|$. In this limit we will find the double logarithm associated with $P_{Q \rightarrow Q}(z_1)P_{Q \rightarrow Q}(z_2)$, while in the other regions there are those associated with splittings into gluons. Now, the integral in \mathbf{x} is dominated by values much smaller than those dominating the integrals in \mathbf{y}_1 and \mathbf{y}_2 . Neglecting \mathbf{x} with respect to \mathbf{y}_1 and \mathbf{y}_2 , we obtain:

$$\begin{aligned}
\mathbf{M}_{ij}^{(l_2 l_1)} &\simeq I(z_1 z_2 p^-, \mathbf{q}) \frac{1}{(2\pi)^2} \int d^2 \mathbf{y}_1 \frac{\mathbf{y}_{1i}}{(\mathbf{y}_1)^2} e^{-i\mathbf{l}_1 \cdot \mathbf{y}_1} e^{iz_2(1-z_1) \left(\frac{bc}{|\mathbf{y}_1}\right)^n} \\
&\quad \times \frac{1}{(2\pi)^2} \int d^2 \mathbf{y}_2 \frac{\mathbf{y}_{2j} + B\mathbf{y}_{1j}}{(\mathbf{y}_2 + B\mathbf{y}_1)^2 + A\mathbf{y}_1^2} e^{-i\mathbf{l}_2 \cdot \mathbf{y}_2} e^{i(1-z_2) \left(\frac{bc}{|\mathbf{y}_2}\right)^n}. \tag{C.1}
\end{aligned}$$

A double logarithm can be obtained only if the amplitude behaves like $|\mathbf{M}_{ij}| \sim \frac{1}{|\mathbf{l}_1|} \frac{1}{|\mathbf{l}_2|}$. In turn, this means that we must look for the situation in which the integrand behaves like $\frac{\mathbf{y}_{1i}}{|\mathbf{y}_1|^2} \frac{\mathbf{y}_{2j}}{|\mathbf{y}_2|^2}$, which

is true only if the \mathbf{y}_1 integral is dominated by much smaller values than those dominating the \mathbf{y}_2 integral. This will happen if and only if $|\mathbf{l}_1| \gg |\mathbf{l}_2|$. We conclude that the gluon emitted closer to the shock wave must have a larger transverse momentum. We will come back to this later, when we generalize to an arbitrary number of gluons.

Thus for $|\mathbf{l}_1| \gg |\mathbf{l}_2|$, we can neglect \mathbf{y}_1 with respect to \mathbf{y}_2 in the integrand, and the last integral factorizes giving:

$$\mathbf{M}_{ij}^{(l_2 l_1)} \simeq I(z_1 z_2 p^-, \mathbf{q}) \mathbf{f}_i(l_1^-, \mathbf{l}_1) \mathbf{f}_j(l_2^-, \mathbf{l}_2) \quad (|\mathbf{l}_1| \gg |\mathbf{l}_2|),$$

where \mathbf{f}_i is the gluon emission factor introduced in Eq. (5.9). After squaring and integrating in \mathbf{l}_1 and \mathbf{l}_2 , this gives a double logarithm of $\mu_F(q)$.

For completeness let us verify explicitly that the contribution from the region $|\mathbf{l}_1| \ll |\mathbf{l}_2|$ is subdominant. One can show that the amplitude depends on \mathbf{l}_1 and \mathbf{l}_2 as follows:

$$\mathbf{M}_{ij}^{(l_2 l_1)} \propto \begin{cases} \frac{\mathbf{l}_j \mathbf{l}_i}{|\mathbf{l}_2|^4} & \text{if } |\mathbf{l}_1| \ll |\mathbf{l}_2| \ll b_c^{-1} \\ b_c^{\frac{n}{n+1}} \left(\frac{1}{|\mathbf{l}_2|}\right)^{1+\frac{1}{n+1}} \log\left(\frac{|\mathbf{l}_2|^{\frac{1}{n+1}}}{|\mathbf{l}_1| b_c^{\frac{n}{n+1}}}\right) & \text{if } |\mathbf{l}_1| \ll b_c^{-1} \ll |\mathbf{l}_2| \\ \frac{\mathbf{l}_i \mathbf{l}_j}{|\mathbf{l}_1|^4} \left(\frac{|\mathbf{l}_1|}{|\mathbf{l}_2|}\right)^{\frac{1}{n+1}} & \text{if } b_c^{-1} \ll |\mathbf{l}_1| \ll |\mathbf{l}_2| \end{cases}.$$

It is immediate to see that from each of the three regions we only get single logarithms.

Thus, the region $|\mathbf{l}_2| < |\mathbf{l}_1| < |\mathbf{q}|$ dominates, and in the LLA we get:

$$\int \int d^2 \mathbf{l}_1 d^2 \mathbf{l}_2 |\mathbf{M}_{ij}^{(l_2 l_1)}|^2 \approx \frac{1}{2} |I(z_1 z_2 p^-, \mathbf{q})|^2 \left\{ \pi \log \frac{\mu_F(q)^2}{\mu^2} \right\}^2,$$

where the $\frac{1}{2}$ factor comes from the $\theta(|\mathbf{l}_1| - |\mathbf{l}_2|)$.

The second diagram in Fig. 10 is the same with $l_1 \leftrightarrow l_2$. Since the leading contributions come from integration over different regions of transverse momenta, in the LLA there is no interference between the two diagrams. Putting all together and including also the double logarithms arising from the regions $|\mathbf{q}| \gg |\mathbf{q} - \mathbf{l}_1|, |\mathbf{l}_2|$ and $|\mathbf{q}| \gg |\mathbf{l}_1|, |\mathbf{q} - \mathbf{l}_2|$, which can be computed in a similar way, we finally obtain:

$$\begin{aligned} \frac{d\hat{\sigma}_{\text{NLO}}}{d^2 \mathbf{q} dz_1 dz_2} \simeq & \frac{1}{4\pi^2} \left\{ |\tilde{I}(z_1 z_2 p^-, \mathbf{q})|^2 P_{Q \rightarrow Q}(z_1) P_{Q \rightarrow Q}(z_2) + |\tilde{I}((1 - z_2)p^-, \mathbf{q})|^2 P_{Q \rightarrow g}(1 - z_2) P_{Q \rightarrow Q}(z_1) \right. \\ & \left. + |\tilde{I}(z_2(1 - z_1)p^-, \mathbf{q})|^2 P_{Q \rightarrow g}(1 - z_1) P_{Q \rightarrow Q}(z_2) \right\} \frac{1}{2!} \left[\frac{\alpha_s}{2\pi} \log \frac{\mu_F^2(q)}{\mu^2} \right]^2. \end{aligned}$$

which shows that the optimal factorization scale is $\mu_F(q)$.

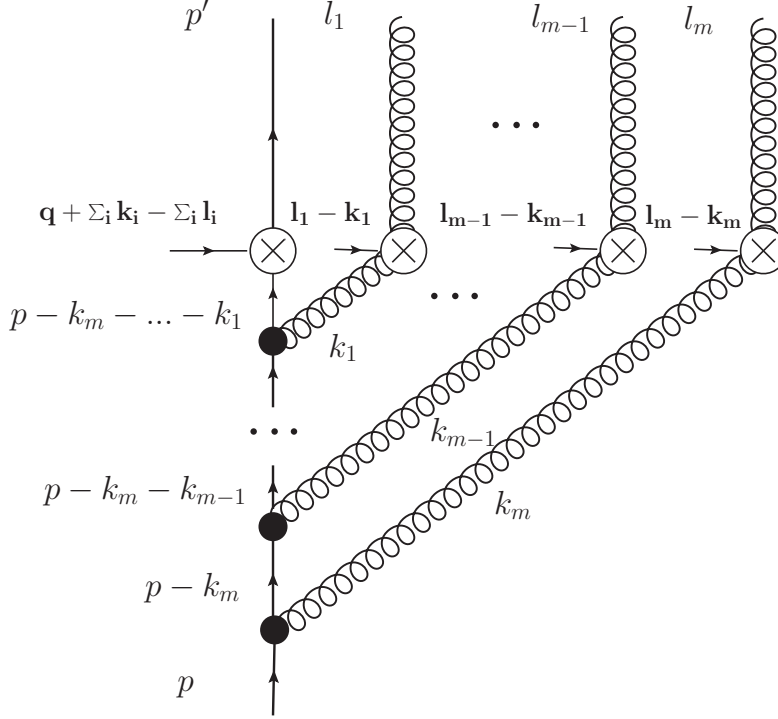


Figure 11: *Typical relevant diagram for the emission of m gluons.*

Generalization to an arbitrary number m of emitted gluons is straightforward. Consider the typical relevant diagram shown in Fig. 11, and let us look at the transverse momenta involved in the quark-gluon vertices. In the first one from below only \mathbf{k}_m appears, thus the contribution to the amplitude will be $\frac{\mathbf{k}_m \cdot \boldsymbol{\varepsilon}_m}{|\mathbf{k}_m|^2}$, like in the case of one gluon emission. In the next vertex both \mathbf{k}_m and \mathbf{k}_{m-1} are involved, but it is obvious that its contribution should reduce to $\frac{\mathbf{k}_{m-1} \cdot \boldsymbol{\varepsilon}_{m-1}}{|\mathbf{k}_{m-1}|^2}$ when $|\mathbf{k}_m| \ll |\mathbf{k}_{m-1}|$. This is true for all the m vertices: if the transverse momentum \mathbf{k} of a gluon is much larger than those of the gluons which were emitted previously, then its contribution to the amplitude will be $\frac{\mathbf{k} \cdot \boldsymbol{\varepsilon}}{|\mathbf{k}|^2}$. Thus in general we can write, for the diagram in Fig. 11:

$$M^{(l_m \dots l_1)} = -2^{m+1} p'^- (ig_s)^m \mathbf{M}_{i_1 \dots i_m}^{(l_m \dots l_1)} \prod_{j=1}^m (\boldsymbol{\varepsilon}_j)_{i_j},$$

where:

$$\mathbf{M}_{i_1 \dots i_m}^{(l_m \dots l_1)} = \int \left(\prod_{j=1}^m \frac{d^2 \mathbf{k}_j}{(2\pi)^2} \right) \left(\prod_{j=1}^m \frac{(\mathbf{k}_j + \sum_{r>j} \mathcal{O}(\mathbf{k}_r))_{i_j}}{\mathbf{k}_j^2 + \sum_{r>j} \mathcal{O}(\mathbf{k}_j \cdot \mathbf{k}_r) + \sum_{r,s>j} \mathcal{O}(\mathbf{k}_s \cdot \mathbf{k}_r)} \right) \times \\ \times I(z_1 z_2 p^-, \mathbf{q} + \sum_{j=1}^m (\mathbf{k}_j - \mathbf{l}_j)) \times \left(\prod_{j=1}^m I(l_j^-, \mathbf{l}_j - \mathbf{k}_j) \right).$$

Fourier-transforming this expression and considering the limit $|\mathbf{q}| \gg |\mathbf{l}_j|$ ($j = 1, \dots, m$), we would obtain an expression analogous to (C.1) with m integrals instead of two. From the structure of the amplitude in \mathbf{k} space, it is clear that it will be:

$$\mathbf{M}_{i_1 \dots i_m}^{(l_m \dots l_1)} \simeq I(z_1 z_2 p^-, \mathbf{q}) \frac{1}{(2\pi)^{2m}} \int \left(\prod_{j=1}^m d^2 \mathbf{y}_j e^{-i \mathbf{l}_j \mathbf{y}_j} e^{i \frac{l_j^-}{p^-} \left(\frac{b_c}{|\mathbf{y}_j|} \right)^n} \right) \Psi(\mathbf{y}_1, \dots, \mathbf{y}_m),$$

where the multi-particle wavefunction Ψ :

$$\Psi(\mathbf{y}_1, \dots, \mathbf{y}_m) \simeq \prod_{j=1}^m \frac{(\mathbf{y}_j)_{i_j}}{(\mathbf{y}_j)^2} \quad \text{if} \quad |\mathbf{y}_1| \ll |\mathbf{y}_2| \ll \dots \ll |\mathbf{y}_m|.$$

This means that the only term with m^{th} power of a large logarithm comes from the region $|\mathbf{l}_1| \gg |\mathbf{l}_2| \gg \dots \gg |\mathbf{l}_m|$. When computing the total cross section with m identical gluons in the final state, we can always reorder the gluons so that $|\mathbf{l}_1| > |\mathbf{l}_2| > \dots > |\mathbf{l}_m|$. Then in the LLA only the shown diagram contributes, with a $\frac{1}{m!}$ factor from $\theta(|\mathbf{l}_{\text{close}}| > \dots > |\mathbf{l}_{\text{far}}|)$. Putting all together, we get

$$\frac{d\hat{\sigma}_{\text{NLO}}}{d^2 \mathbf{q}} \simeq \frac{1}{4\pi^2} |\tilde{I}(p^- \prod_{j=1}^m z_j, \mathbf{q})|^2 \prod_{j=1}^m P_{Q \rightarrow Q}(z_j) dz_j \frac{1}{m!} \left[\frac{\alpha_s}{2\pi} \log \frac{\mu_F^2(q)}{\mu^2} \right]^m,$$

where:

$$z_j = 1 - \sum_{i=j}^m l_i^- / p^-.$$

All these large logarithms are absorbed into the PDF normalized at the scale $\mu_F(|\mathbf{q}|)$.

References

- [1] G. 't Hooft, ‘‘Graviton Dominance in Ultrahigh-Energy Scattering,’’ Phys. Lett. B **198**, 61 (1987).
- [2] T. Banks and W. Fischler, arXiv:hep-th/9906038.

- [3] D. M. Eardley and S. B. Giddings, Phys. Rev. D **66**, 044011 (2002) [arXiv:gr-qc/0201034].
- [4] S. B. Giddings and V. S. Rychkov, Phys. Rev. D **70**, 104026 (2004) [arXiv:hep-th/0409131].
- [5] D. Amati, M. Ciafaloni and G. Veneziano, Phys. Lett. B **197**, 81 (1987).
- [6] H. L. Verlinde and E. P. Verlinde, Nucl. Phys. B **371**, 246 (1992) [arXiv:hep-th/9110017].
- [7] D. N. Kabat and M. Ortiz, Nucl. Phys. B **388**, 570 (1992) [arXiv:hep-th/9203082].
- [8] D. Amati, M. Ciafaloni and G. Veneziano, Int. J. Mod. Phys. A **3**, 1615 (1988),
Nucl. Phys. B **347**, 550 (1990).
- [9] D. Amati, M. Ciafaloni and G. Veneziano, Phys. Lett. B **289**, 87 (1992),
Nucl. Phys. B **403**, 707 (1993), JHEP **0802**, 049 (2008) [arXiv:0712.1209 [hep-th]].
- [10] M. Ciafaloni and D. Colferai, JHEP **0811**, 047 (2008) [arXiv:0807.2117 [hep-th]].
- [11] G. Veneziano and J. Wosiek, JHEP **0809**, 023 (2008) [arXiv:0804.3321 [hep-th]].
JHEP **0809**, 024 (2008) [arXiv:0805.2973 [hep-th]].
- [12] S. B. Giddings, D. J. Gross and A. Maharana, Phys. Rev. D **77**, 046001 (2008)
[arXiv:0705.1816 [hep-th]]; S. B. Giddings and M. Srednicki, Phys. Rev. D **77**, 085025 (2008)
[arXiv:0711.5012 [hep-th]]; S. B. Giddings and R. A. Porto, arXiv:0908.0004 [hep-th].
- [13] N. Arkani-Hamed, S. Dimopoulos and G. R. Dvali, Phys. Lett. B **429**, 263 (1998) [arXiv:hep-ph/9803315];
I. Antoniadis, N. Arkani-Hamed, S. Dimopoulos and G. R. Dvali, *ibid.* **436**, 257 (1998) [arXiv:hep-ph/9804398];
- [14] S. B. Giddings and S. Thomas, Phys. Rev. D **65**, 056010 (2002) [arXiv:hep-ph/0106219];
S. Dimopoulos and G. Landsberg, Phys. Rev. Lett. **87**, 161602 (2001) [arXiv:hep-ph/0106295].
- [15] G. F. Giudice, R. Rattazzi and J. D. Wells, “Transplanckian collisions at the LHC and beyond,” Nucl. Phys. B **630**, 293 (2002) [arXiv:hep-ph/0112161].
- [16] J. L. Feng and A. D. Shapere, Phys. Rev. Lett. **88**, 021303 (2002) [arXiv:hep-ph/0109106].
L. Anchordoqui and H. Goldberg, Phys. Rev. D **65**, 047502 (2002) [arXiv:hep-ph/0109242].
- [17] R. Emparan, M. Masip and R. Rattazzi, “Cosmic rays as probes of large extra dimensions and TeV gravity,” Phys. Rev. D **65**, 064023 (2002) [arXiv:hep-ph/0109287].

- [18] D. V. Gal'tsov, G. Kofinas, P. Spirin and T. N. Tomaras, “Transplanckian bremsstrahlung and black hole production,” arXiv:0908.0675 [hep-ph].
- [19] P. C. Aichelburg and R. U. Sexl, “On the gravitational field of a massless particle,” Gen. Rel. Grav. **2**, 303 (1971).
- [20] see ‘Gravity in Flat Extra Dimensions’ in C. Amsler *et al.* [Particle Data Group], Phys. Lett. B **667**, 1 (2008)
- [21] M. Sjodahl and G. Gustafson, Eur. Phys. J. C **53**, 109 (2008) [arXiv:hep-ph/0608080].
- [22] J. I. Illana, M. Masip and D. Meloni, Phys. Rev. D **72**, 024003 (2005) [arXiv:hep-ph/0504234].
- [23] V. S. Rychkov, Phys. Rev. D **70**, 044003 (2004) [arXiv:hep-ph/0401116].
- [24] S. Weinberg, *The Quantum theory of fields. Vol. 1*, Cambridge Univ. Pr., 1995
- [25] J. I. Illana, M. Masip and D. Meloni, Phys. Rev. Lett. **93**, 151102 (2004) [arXiv:hep-ph/0402279].
- [26] L. Lonnblad and M. Sjodahl, JHEP **0610**, 088 (2006) [arXiv:hep-ph/0608210].
- [27] R. K. Ellis, W. J. Stirling and B. R. Webber, *QCD and collider physics*, Cambridge Univ. Pr., 1996.
- [28] F. Ambrogini *et al.*, “Proceedings of the Workshop on Monte Carlo’s, Physics and Simulations at the LHC PART I,” arXiv:0902.0293 [hep-ph].
- [29] N. D. Birrell and P. C. W. Davies, *Quantum Fields In Curved Space*, Cambridge Univ. Pr., 1982.
- [30] S. Weinberg, “Dynamics at infinite momentum,” Phys. Rev. **150**, 1313 (1966).
For a review see e.g. www.lpthe.jussieu.fr/~salam/repository/docs/thesis.ps.gz.
- [31] J. D. Bjorken, J. B. Kogut and D. E. Soper, “Quantum Electrodynamics At Infinite Momentum: Scattering From An External Field,” Phys. Rev. D **3**, 1382 (1971).
- [32] A. Hebecker, “Diffraction in deep inelastic scattering,” Phys. Rept. **331**, 1 (2000) [arXiv:hep-ph/9905226].
- [33] V. V. Kiselev, Phys. Rev. D **58**, 054008 (1998) [arXiv:hep-ph/9710432].

- [34] Y. V. Kovchegov and K. Tuchin, Phys. Rev. D **74**, 054014 (2006) [arXiv:hep-ph/0603055].
- [35] J. C. Collins, D. E. Soper and G. Sterman, Nucl. Phys. B **261**, 104 (1985).